

## **F-111 Stiffener Run Out #2 Parametric Study**

J. Paul

DSTO-TN-0104

20000105 011

# F-111 Stiffener Run Out #2 Parametric Study

*J. Paul*

**Airframes and Engines Division  
Aeronautical and Maritime Research Laboratory**

DSTO-TN-0104

## ABSTRACT

The Royal Australian Air Force (RAAF) currently has in service a fleet of F-111 aircraft. The conditions under which the RAAF operates these aircraft have proved to be conducive to cracking in the structurally critical wing pivot fitting, and certification testing in the cold proof load test has demonstrated failures at that location. The RAAF has contracted Lockheed Martin Tactical Aircraft Systems (LMTAS) to perform a Durability And Damage Tolerance Analysis on the aircraft. One control point of concern, in this report, is the Stiffener Run Out Number 2 in the wing pivot fitting. The Aeronautical and Maritime Research Laboratory (AMRL) developed a bonded boron/epoxy reinforcement to reduce the high plastic strains in this critical region, and as a result has significant experience in analysing this region. LMTAS, in conjunction with the RAAF, requested that the AMRL perform an elastic and plastic stress analysis of Stiffener Run Out Number 2 including the effect of varying the geometric parameters associated with it.

## RELEASE LIMITATION

*Approved for public release*

DEPARTMENT OF DEFENCE  
DEFENCE SCIENCE & TECHNOLOGY ORGANISATION **DSTO**

*Published by*

*DSTO Aeronautical and Maritime Research Laboratory  
PO Box 4331  
Melbourne Victoria 3001 Australia*

*Telephone: (03) 9626 7000  
Fax: (03) 9626 7999  
© Commonwealth of Australia 1999  
AR-010-301  
October 1999*

**APPROVED FOR PUBLIC RELEASE**

# F-111 Stiffener Run Out #2 Parametric Study

## Executive Summary

The conditions under which the RAAF operate the F-111 aircraft are conducive to cracking in the structurally critical wing pivot fitting, and certification testing in the Cold Proof Load Test (CPLT) has demonstrated such failures. One region of concern is the Stiffener Run Out Number 2 (SRO#2) in the wing pivot fitting. In order to calculate a safe inspection interval, a detailed knowledge of the elastic and residual stress field is required for this location.

Classical plasticity solution techniques reveal severe limitations in representing material behaviour under non-symmetric cyclic loading. As a result, AMRL previously researched and developed an alternative constitutive material model which would provide an improved representation of the residual stress field after a CPLT-type load cycle. That constitutive model was used for the current analyses of SRO#2. This report outlines the detailed geometric parametric study undertaken on SRO#2. Elastic and plastic finite element analyses of SRO#2 were performed for a matrix of local geometric parameter values typical of the fleet variability. The plastic analyses determined residual stresses after the application of a CPLT cycle.

The results of the analyses presented have been used by Lockheed Martin Tactical Aircraft Systems (LMTAS) to provide the RAAF with new improved inspection intervals for the SRO#2 region in the wing pivot fitting, with and without the external AMRL boron doubler.

## Authors



### Julian Paul Airframes and Engines Division

*Mr Paul has a degree in Aeronautical Engineering and a Masters in Mechanical Engineering in the repair of thick composite structures. He has worked in the finite element field for 13 years providing AMRL with a high level of expertise in the area of computational analysis which has been utilised to solve a variety of RAAF related stress/strain problems seen on the F-111 and F/A-18 aircraft. He is currently the Functional Head of the Computational Stress Analysis Facilities within AED and leads the team working on the F-111 Structural Integrity Task, which provides the residual stress input required for the calculation of the inspection interval for the Fuel Flow Vent Hole #13 location in the F-111 Wing Pivot Fitting. Author's CV*

---

---

## Contents

1. INTRODUCTION.....	1
2. PARAMETER DETERMINATION .....	2
3. NUMERICAL TECHNIQUES: UNIFIED CONSTITUTIVE MODEL .....	3
4. FINITE ELEMENT MODELS .....	4
4.1 Calibration.....	6
4.2 Calibration Results .....	7
4.2.1 Unreinforced .....	7
4.2.2 Reinforced .....	7
5. PARAMETRIC STUDY RESULTS .....	8
6. CONCLUSIONS.....	8
7. ACKNOWLEDGMENTS.....	9
8. REFERENCES .....	10
APPENDIX A:TABLES .....	11

## 1. Introduction

The Royal Australian Air Force (RAAF) currently has in service a fleet of General Dynamics<sup>1</sup> (LMTAS) F-111 aircraft. The conditions under which the RAAF operates this aircraft have been shown to be conducive to cracking in the structurally critical Wing Pivot Fitting (WPF), and certification testing in the Cold Proof Load Test (CPLT) has demonstrated failure in the same region. CPLT involves the application of limit loads to the aircraft at -40° C. The load cycle is defined by the particular Structural Integrity Program (SIP) currently in action<sup>2</sup>. SIP III results in a -2.4 g, 7.33 g, -3.0 g, 7.33 g load applied to the aircraft. A critical area of the WPF in which in-service fatigue cracking has been observed is at the integral stiffeners on the upper surface of the WPF where they run out at the outer bulkhead of the WPF. Indeed, CPLT failure has occurred at the Stiffener Runout No. 2 (see Reference 1 and Figure 1).

The Aeronautical and Maritime Research Laboratory (AMRL) was assigned the task of devising a solution to prevent further problems in this critical region during CPLT, and the resultant modification to the WPF was a local boron/epoxy uniaxial laminate reinforcement (doubler), the details of which are discussed in Reference 1.

The RAAF contracted LMTAS to undertake a Durability And Damage Tolerance Analysis (DADTA) on fatigue critical areas of the F-111, including the WPF Stiffener Run Out No. 2 (SRO #2), DADTA Item 92. The Damage Tolerance philosophy currently employed on the SRO #2 requires a confidence cut of 0.005" (0.13mm) after each inspection which corresponds to the notional RAAF confidence limit of the current magnetic rubber inspection technology in detecting a crack in this region. The technique used to perform the confidence cut is inaccurate and as a result the fleet has a wide variation in SRO geometries. In addition, the initial starting geometries for each aircraft were different due to the manufacturing process and fatigue cracks have been cut out from many run outs. In order to perform the DADTA LMTAS required the stress versus load response, both with and without doubler and with various grind out configurations. A matrix of geometric parameters and their ranges was developed from inspection data provided from the RAAF and is presented in this report and in Reference 2. The SRO #2 configurations to be analysed by LMTAS in the DADTA were determined from the parametric study results.

The SRO #2 undergoes gross plastic yielding when subjected to the CPLT loading. Classical techniques of modelling the plastic behaviour of materials have inherent difficulties in representing the high inelastic strain behaviour under cyclic loading. As a result of these limitations, AMRL has developed and utilised a set of constitutive equations to model non-linear material behaviour [3] and has implemented these

---

<sup>1</sup> Lockheed Martin Tactical Aircraft Systems (LMTAS) was formerly Lockheed Fort Worth Company which was formerly General Dynamics.

<sup>2</sup> SIP III indicated that the F-111 aircraft has undergone three CPLT's over its life.

equations into the PAFEC Finite Element Package [4]. This unified constitutive law was used to analyse the configurations in the parametric study that exhibited yielding.

This report presents the methodology used by AMRL to calculate the stress/strain fields for the geometric parametric study on the SRO #2. The finite element models were calibrated against two full scale tests under CPLT loading. The unreinforced models were calibrated against the USAF CPLT [5], while the reinforced models were calibrated against aircraft A8-113 CPLT conducted in September 1990 [6]. The results of the extensive calibration of the finite element models are also presented.

## 2. Parameter Determination

As part of the RAAF's damage tolerance philosophy in maintaining the F-111 aircraft, the RAAF perform a confidence cut of 0.005" (0.13mm). This confidence cut results in the fleet of aircraft having significantly varying SRO #2 geometries. The initial parameters studied in the parametric analysis were driven by the changing local geometric parameters. Over the past twelve months, AMRL has been collating F-111 wing inspection data provided by the RAAF. The full details of this collation can be found in Reference 2, however for the purposes of determining the initial parametric configurations to be analysed, AMRL focused on:

- a) reinforced and unreinforced wings,
- b) SRO grind out depths,
- c) SRO grind out radii, and
- d) local WPF plate thicknesses.

During the calibration process of the reinforced wing (A8-113), it was determined that, for the reinforced configuration, the local geometric 'kink' angle (see Figure 2), has a significant influence on the bending field in the SRO (see Section 4.2.2). The inclusion of the 'kink' angle, for the reinforced analyses, results in a reduction in the residual stresses calculated after the application of the CPLT loads.

The parameter values in the analysis matrix analysed were directly based on the fleet inspection data collected by the RAAF. As noted in [2], these data have a low degree of reliability, however they are the only data currently available. The complete inspection data for the relevant parameters, as at August 1993, are presented in tabular form in Table 1. The histograms developed from this inspection data for minimum plate thickness, SRO grind out radius, SRO height and 'kink' angle are presented in Figures 3 to 6. The resultant base analysis matrix developed is shown in Table 2. The initial stiffener height of 0.3689" (9.37mm) was obtained from Reference 7 and is slightly higher than the actual nominated drawing height. It is worth noting that the worst case scenario for this matrix may actually never be achieved in the fleet, however these

points were included in order to investigate the full effects of varying all parameters in the matrix.

The geometric configuration was based upon the virgin wing specifications [7] and the matrix of configurations shown in Table 2 were analysed for each of the conditions outlined below:

Doubler:	No doubler and doubler
Elastic Load Condition:	7.33 g, -2.4 g and -3 g.
Plastic Load Condition:	III-SIP
Plate Thickness:	0.325" (8.26mm), 0.2894" (7.35mm), 0.260" (6.60mm)
'kink' angle:	1.33° (only the doubler configuration utilised this parameter.)

The no grind out condition (ie. virgin wing) has the following WPF geometric values:

Plate thickness:	7.35 mm (0.2894")
Max. stiffener depth:	49.02 mm (1.9300")
Min. stiffener depth:	9.37 mm (0.3689")
Stiffener thickness:	5.00 mm (0.1969")

### 3. Numerical Techniques: Unified Constitutive Model

Classical techniques of modelling plasticity have a high degree of accuracy provided the inelastic strains are kept small. However, they become increasingly inaccurate when the material exhibits high inelastic strains and, in addition, undergoes cyclic loading that causes gross plastic yielding. The current problem area in the F-111 is SRO #2 which experiences the two previously mentioned phenomena and therefore, using classical techniques, would lead to a high degree of inaccuracy.

The Unified Constitutive model, originally developed by Ramaswamy [8], is based upon the generic back stress and drag stress model proposed by Bodner and Stouffer [9]. Over the past 5 years AMRL has utilised and developed [3] these constitutive equations to model non-linear material behaviour in aluminium, adhesive and steels. The algorithms have been implemented into the PAFEC Finite Element Package [4] enabling practical problems to be solved.

In order to represent the D6ac steel material of the F-111 WPF correctly in the high strain, cyclic loading regime, experimental stress/strain data were obtained from coupon tests [10], at room temperature. The experimental stress/strain curve under a loading of III SIP was compared with one generated using the Unified Constitutive model (see Figure 7) and one generated using classical plasticity (see Figure 8). From these two figures it is clear that classical plasticity cannot adequately represent the

material behaviour under cyclic loading, and as the strain level is increased so too is the error.

The original implementation of the Unified Constitutive model in PAFEC, as detailed in Reference 4, was based upon three dimensional elements. The finite element work performed in this report was in two dimensions, so the appropriate modification to the code was performed. Unfortunately a known problem with the current set of equations is the time step algorithm. AMRL has recently developed a modified solution technique [11] that solves this time step problem, however this was unavailable at the time of performing this work. The initial F-111 SRO#2 solution ran 64 hours on a HP9000-750 Unix machine and had performed only a fraction of the total solution time. This clearly was unacceptable as the parametric matrix was quite extensive. The decision was taken to perform the finite element structural analysis using classical plasticity and then to derive the stresses from the analysis strain output using the Unified Constitutive model. The solution to this problem is based upon the fact that the total strains for the classical solution are accurate, however the stresses are not. The total strain fields were validated against the calibration results from real aircraft data, see Section 4.1. An interface program was written to provide the external Unified Constitutive model code with the total strain history from the classical solution for every node in the section of interest in the structure. The Unified Constitutive model then produced the corresponding stress histories. The plastic stress solution obtained followed the material behaviour previously shown in Figure 7.

## 4. Finite Element Models

The two dimensional finite element model used in this analysis was originally developed in References 1 and 7. The local geometry of the SRO region was modified for each configuration in the parametric matrix. There were 36 models incorporating the geometric configurations for each of the 7 analysis cases. Table 3 describes the data file names with a description of each data file's parameters which were analysed. The -3.0  $g$  loading condition was additionally analysed, however because this load condition is elastic the data file descriptions and subsequent results are not presented in this report. The 1.33° 'kink' angle data file's parameters are identical to the 0° 'kink' angle files however the naming convention has a 'K3' added in the data file name. The 0° 'kink' angle data were also not presented. A FORTRAN program was used to generate the modified 1.33° 'kink' angle structure.

The data file naming convention for all the finite element models is described below:

F111	- Base Name
P	- Plastic analysis
E	- Elastic analysis
U	- Unrepaired ie. no doubler
R	- Repaired ie. doubler
-	- 7.33 g Load or III SIP
2	- -2.4 g Load
3	- -3.0 g Load
-	- 'kink' angle = 0°
K3	- 'kink' angle = 1.33°
	<u>Grind out Radius</u> <u>Grind out Depth</u>
-	- 0.1575" 0.000"
A	- 0.4500" 0.0500"
B	- 0.4500" 0.1089"
C	- 0.4500" 0.1689"
D	- 0.4500" FULL
E	- 0.7800" 0.0500"
F	- 0.7800" 0.1089"
G	- 0.7800" 0.1689"
H	- 0.7800" FULL
I	- 1.0000" 0.0500"
J	- 1.0000" 0.1089"
K	- 1.0000" 0.1689"
-	- Plate Thickness = 0.2894"
P1	- Plate Thickness = 0.3250"
P2	- Plate Thickness = 0.2600"
NFL	- Unified Constitutive model data file.

additionally the calibration models described in Section 4.1 have the naming convention:

F111LMP	- USAF unrepaired plastic model [1]
F113ER	- A8-113 repaired elastic model [12]

The finite element virgin mesh geometry of the SRO #2 region can be seen in Figure 9. The various grind out geometries can be seen in Figures 10 to 20. Figures 21 and 22 show these localised geometries superimposed onto each other.

Many intermediate analyses, such as the 0° 'kink' angle runs, calibration test configurations, etc., are not presented in this report. Even though the data from those runs were essential to obtaining the final results for this analysis the data are not used in the results.

#### 4.1 Calibration

Prior to performing the parametric analysis a detailed calibration of the unreinforced and reinforced models was required in order to validate the calibration constants used. The unreinforced finite element models were deemed to be calibrated when the bending to axial ratio between the strain in the SRO (gauge 9L [7]) and the strain at the top surface plate (gauge 6L [7]) was in agreement with the experimental test data. For the plastic analyses of the unreinforced models this calibration took place at 50% of load where the strains were assumed to be elastic. Likewise, for the reinforced models, the bending to axial ratios were calculated from the SRO peak strain (gauge LWS32 [12]) and the strain on the top surface of the boron/epoxy doubler (gauge PFD5 [12]). In addition, the bottom surface plate stress (gauge LWR10 [12]) was used as an supplementary check due to the amount of adhesive shear lag which would affect the strain reading at gauge PFD5. The definitions of bending and axial strains are given below:

$$\begin{aligned}\text{Axial Strain} &= ([\text{gauge 6L or PFD5}] \text{ Strain} + [\text{gauge 9L or LWS32}] \text{ Strain}) / 2 \\ \text{Bending Strain} &= \text{Axial Strain} - [\text{gauge 6L or PFD5}] \text{ Strain} \\ \text{Ratio} &= \text{Bending Strain} / \text{Axial Strain}\end{aligned}$$

The calibration technique described above was a LMTAS requirement.

The finite element models contained 2 spring elements which were used to allow calibration of the secondary bending effects seen in the wing tests (see Reference 1 for more details). These spring stiffnesses are referred to as the calibration constants throughout this report.

The unreinforced models were calibrated from the USAF strain survey [13] and two sets of calibration constants were developed for the 7.33 g and -2.4 g load cases. These constants were applied to the elastic unreinforced analyses (data file series F111EU and F111EU2). For the plastic analysis the 7.33 g elastic calibration constants were used throughout the CPLT load cycle. The finite element mesh used and gauge locations 6L and 9L are shown in Figure 23.

The reinforced models were calibrated from the recent CPLT of the A8-113 aircraft [12]. The left hand wing A15-9 data was used. Again two sets of calibration constants were developed for the up and down loading. The finite element mesh used and gauge locations LWS32, PFD5 and LWS10 are shown in Figure 24. After initially obtaining unsatisfactory calibration results, it was determined that the current geometric parameters chosen were not sufficient to provide the correct bending ratio in the SRO region. The parameter 'kink' angle was introduced into the analysis and then obtained from the RAAF doubler application report for the A8-113 left hand wing.

Another adjustment was required to be made to the model, because the bending mode of the upper surface of the boron/epoxy doubler was inconsistent with the measured

strain gauge data. This effect is caused by the large softening area at the step zone (see Figure 2). Previous work [7] tailored the boron/epoxy doubler and adhesive shapes in this region. The finite element model provided no stiffness variation in this region in the adhesive peel direction. A spring element was added to this region so as to model the effect of the adhesive and to take into account the variation of the doubler thickness due to fill<sup>3</sup> plies being added in the doubler manufacturing process.

After including all the local phenomena in the analysis, good agreement was obtained with the experimental strain gauge data. The finite element model with a 'kink' angle of 1.97° (determined from Table 1 for wing A15-9) is shown in Figure 25.

After the effect of the 'kink' angle on the reinforced calibration model had been evaluated, each configuration of the unreinforced model was re-analysed with the same geometric modification. The effect of this parameter was determined to be a localised effect on only the reinforced models, due to the doubler and therefore the parameter was not used in the unreinforced models.

## 4.2 Calibration Results

### 4.2.1 Unreinforced

The unreinforced finite element analysis was calibrated from the USAF strain survey [13] for both the elastic and plastic analyses. The plastic analysis results, for strain gauge location 9L are shown in a plot of the strain versus load response for both the USAF wing and the finite element mesh (see Figure 26). In this Figure a 100% up load is equivalent to 7.26 g and 100% down load is equivalent to -2.38 g. The elastic model calibration results are based upon the calculated bending to axial ratio, previously discussed, and are shown in Table 4. Good agreement was obtained between the measured strain gauge data and the finite element model. In the plastic analysis the calibration constants were not changed during the application of the cyclic load and the positive 'g' load calibration constants were utilised.

### 4.2.2 Reinforced

The reinforced finite element analysis was calibrated from the CPLT of the A8-113 aircraft [12]. The geometry for this wing was obtained from the MAG rubber inspection performed by the RAAF and supplemented with additional measurements requested from the RAAF by AMRL. From the CPLT results the left hand wing of A8-113 showed a slightly higher SRO strain than the right and was therefore chosen as the base line for the calibration process. The SRO strain was below the yield point of the material, however in the parametric study it was found that some configurations of

---

<sup>3</sup>Fill plies are alternate layers of boron and adhesive that are added at the manufacturing stage so that the upper doubler will remain horizontal. This process eliminates any possibility of a 'kink' occurring in the fibres of the upper doubler.

the SRO analysed do extend beyond the yielding stress. The local bending in the region of the SRO, was slightly modified due to the application of the boron/epoxy doubler. This resulted in the unreinforced calibration constants not representing the bending correctly, due to one of the calibration springs being directly under the doubler. The constants were slightly adjusted in order improve the calibration results.

In addition, the boron/epoxy doubler has a large region in the step that is filled with adhesive. A spring element was placed in this region to fine tune the secondary bending of the doubler. The final modification from the unreinforced model was the improved representation of local geometry in the form of the 'kink' angle. Both these points were discussed in detail in Section 4.1.

A selection of results from the various analyses run can be seen in Table 5. The calculations for pairs of gauges PFD5, LW32b and LWR10a, LW32b were designated case 1 and 2 respectively and the difference (DIFF) is relative to those obtained from the A8-113 CPLT. The bold lines are the final acceptable calibration analyses for the reinforced finite element models.

## 5. Parametric Study Results

The calibration work outlined in the previous section was then applied to the parametric analysis configurations. The results of all cases are presented in three forms. The maximum averaged Von Mises<sup>4</sup> stress is provided in Table 3 and these data are then presented as bar graphs of for each configuration block. These graphs can be seen in Figures 27 to 33. The Von Mises stress contour plots for each configuration point that was used in the DADTA were reproduced by LMTAS in Reference 14. These plots illustrate the changing stress distribution, elastic or residual (where applicable), as the SRO #2 geometry changes. The plastic unreinforced classical results were not presented in Reference 14 as the stress distributions are invalid.

## 6. Conclusions

This parametric study on the F-111 Stiffener Run Out Number 2 has shown that several parameters have a significant effect on the stress and residual stress distribution through the stiffener. The most significant parameter that affects the stress and residual stress is the radius of the grind, with the plate thickness also having a secondary effect. The analysis performed on the aircraft with doublers shows that a

---

<sup>4</sup>The maximum average Von Mises stress is calculated as the average of 5 nodes around the peak node. The maximum difference found between this value and the peak value was around 3.5%.

local angle of the plate relative to the skin has a significant effect on the bending field in the local SRO section. This was confirmed in the calibration of aircraft A8-113.

The elastic and residual stress results of this parametric study on the F-111 Stiffener Run Out Number 2 have been used as the stress input to the RAAF DADTA analysis performed by LMTAS [14]. One of the main objectives of the DADTA analysis was to determine the inspection interval for a RAAF F-111 with the AMRL boron/epoxy doubler applied. The stress distributions determined have shown that a dramatic difference in residual stress exists for aircraft with a boron doubler. This result is reflected in the results of the DADTA analysis. For an aircraft with no doubler and worst case scenario of geometry the inspection interval has been predicted at 87 hours, however for the same configuration, but with a doubler, the inspection interval was calculated as 2,000 hours. At the other extreme of good geometry, the inspection interval has been predicted to be 446 hours with no doubler and 6,000 hours with doubler. This result will allow the RAAF to readjust their maintenance schedule and result in dramatic cost saving and increased aircraft availability.

## 7. Acknowledgments

The author wishes to acknowledge the contributions of many people within DSTO, the RAAF, LMTAS and other institutions. The background work required to perform this task extends many years into the past. Thank you to all those people who have worked on this task. Special thanks go to Mr. G. McCabe from AED at DSTO for his help in generating all the geometries and Mr. D. Horrigan who worked under contract to the Aeronautical Research Laboratory on this task.

## 8. References

- 1) Molent L. and Jones R, 'Stress analysis of a boron/epoxy reinforcement for the F-111C wing pivot fitting', ARL-STRUC-REP-426, Aeronautical Research Laboratory, DSTO, Melbourne, Australia, May 1987.
- 2) Molent L. and Swanton G., 'A Parametric Survey of Cracking in RAAF F-111C WPF Stiffeners', ARL-TR-55, Aeronautical Research Laboratory, DSTO, Melbourne, Australia, February 1994.
- 3) Bridgford N., 'A Summary of the Bodner-Stouffer Constitutive Model', ARL-STRUC-TM-513, Aeronautical Research Laboratory, DSTO, Melbourne, Australia, May 1989.
- 4) Paul J., Bridgford N. and Stouffer D.C., 'Progress report on the implementation of a constitutive model in the PAFEC Finite Element Package', ARL-STRUC-TM-529, Aeronautical Research Laboratory, DSTO, Melbourne, Australia, June 1990.
- 5) Susans, G.R., Patching, C.A., and Beckett, R.C., 'Visit by an Australian team to the US to discuss the failure of A8-112 during CPLT', Dept. of Defence, AF1511/912/100 Pt3, June 1982.
- 6) Molent L., and Patterson A.K., 'Strain survey of F-111C Aircraft A8-113', ARL-STRUC-TM-585, Aeronautical Research Laboratory, DSTO, Melbourne, Australia, August 1992.
- 7) Jones R, Callinan R.J., Molent L., 'Preliminary design of a boron/epoxy reinforcement for the F-111C wing pivot fitting', ARL-STRUC-REP-429, Aeronautical Research Laboratory, DSTO, Melbourne, Australia, February 1987.
- 8) Ramaswamy V.G., 'A constitutive model for the inelastic Multiaxial cyclic response for a nickel base superalloy Rene 80', NASA Contract Report 3998, July 1986.
- 9) Stouffer D.C. and Bodner S.R., 'A relationship between theory and experiment for a state variable constitutive equation', American Society for Testing and Materials STP, 765, 239-250, 1982.
- 10) Molent, L. and Swanton G., 'F-111 fuel hole #13 strain surveys', ARL-TN-33, Aeronautical Research Laboratory, DSTO, Melbourne, Australia, June 1993.
- 11) Paul J., 'Implementation of a Unified Constitutive Model into the PAFEC Finite Element Package: Final Report', DSTO-TR-0529, Aeronautical and Maritime Research Laboratory, DSTO, Melbourne, Australia, May 1987.
- 12) Molent, L. and Patterson A.K., 'Strain survey of F-111C aircraft A8-113', ARL-STRUC-TM-585, Aeronautical Research Laboratory, DSTO, Melbourne, Australia, August 1992.
- 13) Anon, 'Wing pivot fitting failure investigation. Final crack growth rates and crack growth intervals', General Dynamics, Fort Worth Division, USA, September 1982.
- 14) Dubowski D.M. 'Wing Pivot Fitting Stiffener Number 2 Runout, ARL Stress Analysis Results', Lockheed Fort Worth Company, July 1993.

## Appendix A: Tables

Table 1: F-111C Fleet Inspection data as of August 1993.

NUMBER	WING #	DATE	HOURS	SRO HGT.	SRO THK.	PLATE THICKNESS		RADIUS <sup>1</sup>	'kink' ANGLE <sup>2</sup>
						FWD	AFT		
1	A11-15	930304		0.211	0.159	0.312	0.298	0.910	1.21
2	A11-16	930304		0.141	0.323	0.298	0.291	0.510	0.68
3	A15-3	900925	3824	0.243	0.231	0.225 <sup>3</sup>	0.298	0.750	
4	A15-4	900704	3824	0.213	0.276	0.288	0.270	0.750	1.14
5	A15-5	921108	4388	0.258	0.201	0.318	0.333	0.750	1.36
6	A15-6	921105	4388	0.212	0.209	0.315	0.319	0.710	1.21
7	A15-7	921208	4945	0.292	0.167	0.305	0.302	0.790	
8	A15-8	921215	4945	0.067		0.356	0.297	0.240	
9	A15-9	930111	3747	0.179	0.231	0.288	0.306	0.650	1.97
10	A15-10	930111	3747	0.213	0.220	0.325	0.291	0.700	1.25
11	A15-11	910926		0.200	0.205	0.332	0.325	0.630	
12	A15-12	910926		0.164	0.196	0.315	0.323		
13	A15-289	920210	4414	0.262	0.209	0.321	0.307		
14	A15-14	911114	4146	0.169	0.210	0.324	0.319	0.750	
15	A15-15	900607	2911	0.213	0.242	0.298	0.296	0.980	
16	A15-16	900606	2911	0.217	0.182	0.347	0.290	0.630	
17	A15-19	911023	4387	0.314	0.174	0.288	0.286	0.910	1.25
18	A15-20	911015	4387	0.224	0.206	0.288	0.296	0.590	1.36
19	A15-21	920315	3730	0.161	0.268	0.297	0.302		
20	A15-22	920315	3730	0.154	0.240	0.324	0.309		
21	A15-27	920721	4981	0.216	0.267	0.332	0.286	0.890	
22	A15-28	920710	4981	0.180	0.244	0.284	0.301	0.470	
23	A15-29	861125	3451	0.090	0.298	0.304	0.295	0.980	
24	A15-30	890622		0.177	0.205	0.290	0.293	0.790	
25	A15-35	910929	4535	0.288	0.215	0.292	0.296	1.080	1.21
26	A15-36	910912	4535	0.237	0.217	0.292	0.300	0.850	1.59
27	A15-39	920904	4716	0.245	0.211	0.295	0.283	0.780	1.03
28	A15-40	920904	4716	0.206	0.173	0.287	0.312	0.470	1.36
29	A15-41	910227	3553	0.214	0.238	0.288	0.294	0.780	1.63
30	A15-42	910522	3553	0.215	0.200	0.315	0.303	0.820	1.18
31	A15-43	911127	4234	0.258	0.150	0.320	0.313	0.790	
32	A15-44	911127	4234	0.325	0.185	0.298	0.305	0.830	
33	A15-45	921006	4470	0.150	0.231	0.348	0.311	0.790	
34	A15-46	921105	4470	0.123	0.214	0.329	0.316		
35	A15-47	901207	4513	0.251	0.265	0.295	0.289	0.890	1.40
36	A15-48	910115	4513	0.264	0.199	0.323	0.305	0.750	1.67
37	A15-121	910726	4659	0.254	0.204	0.314	0.291	0.430	
38	A15-122	910726	4659	0.265	0.196	0.309	0.294	0.550	
39	A15-283	910621	4976	0.224	0.201	0.341	0.286	0.410	
40	A15-284	910513	4976	0.221	0.252	0.318	0.298	0.710	
41	A15-295	901004	3966	0.298	0.245	0.297	0.294	0.980	
42	A15-296	901004	3966	0.158	0.214	0.299	0.260	0.790	
43	BA15-1	911217	754	0.253	0.219	0.321	0.294	0.980	
44	BA15-2	911217	754	0.247	0.204	0.285	0.270	0.690	
45	BA15-3	900719	2764	0.201	0.238	0.320	0.315	0.830	1.06
46	BA15-4	900719	2764	0.201	0.235	0.340	0.297	0.980	1.44
47	W47389	900926	4057	0.272	0.198	0.325	0.295	0.980	1.63
48	W47390	901016	4057	0.205	0.199	0.295	0.296	0.530	1.25

All units are in inches, 'kink' angle in degrees, date in yyymmdd.

Blank fields: No inspection data provided by the RAAF.

- 1 Radii readings are the last known measurements as do not necessarily correspond to the Inspection date or Flight hours.
- 2 Only wings with boron/epoxy doublers installed have an associated 'kink' angle measured as part of the doubler application process.
- 3 Wing A15-3, at the time of the initial inspection, had a recorded plate thickness of 0.324 aft and 0.319 fwd and therefore the plate appears to have thinned out between inspections. The data is obviously unreliable.

*Table 2: Base Geometric Configuration Analysis Matrix.*

Stiffener Height	Grind Out Radius		
	.45"	.78"	1.00"
0.3689"			
0.3189"	x	x	x
0.2600"	x	x	x
0.2000"	x	x	x
Full Grind out	x	x	

Table 3: Finite Element Data Structure of Parametric Analysis Matrix.

PLASTIC UNREINFORCED MODELS (CLASSICAL): SIP III				
DATA FILE NAME	GRINDOUT RADIUS (Inches)	STIFFENER HEIGHT (Inches)	PLATE THICKNESS (Inches)	MAX VON MISES <u>RESIDUAL STRESS</u> (ksi)
F111PU	0.1575	0.3689	0.2894	289
F111PUA	0.4500	0.3189	0.2894	243
F111PUB	0.4500	0.2600	0.2894	256
F111PUC	0.4500	0.2000	0.2894	259
F111PUD	0.4500	FULL	0.2894	219
F111PUE	0.7800	0.3189	0.2894	191
F111PUF	0.7800	0.2600	0.2894	199
F111PUG	0.7800	0.2000	0.2894	199
F111PUH	0.7800	FULL	0.2894	175
F111PUI	1.0000	0.3189	0.2894	169
F111PUJ	1.0000	0.2600	0.2894	178
F111PUK	1.0000	0.2000	0.2894	179
F111PUP1	0.1575	0.3689	0.3250	243
F111PUAP1	0.4500	0.3189	0.3250	198
F111PUBP1	0.4500	0.2600	0.3250	207
F111PUCP1	0.4500	0.2000	0.3250	207
F111PUDP1	0.4500	FULL	0.3250	179
F111PUEP1	0.7800	0.3189	0.3250	152
F111PUFP1	0.7800	0.2600	0.3250	156
F111PUGP1	0.7800	0.2000	0.3250	155
F111PUHP1	0.7800	FULL	0.3250	135
F111PUIP1	1.0000	0.3189	0.3250	130
F111PUJP1	1.0000	0.2600	0.3250	135
F111PUKP1	1.0000	0.2000	0.3250	133
F111PUP2	0.1575	0.3689	0.2600	332
F111PUAP2	0.4500	0.3189	0.2600	227
F111PUBP2	0.4500	0.2600	0.2600	267
F111PUCP2	0.4500	0.2000	0.2600	269
F111PUDP2	0.4500	FULL	0.2600	249
F111PUEP2	0.7800	0.3189	0.2600	232
F111PUFP2	0.7800	0.2600	0.2600	246
F111PUGP2	0.7800	0.2000	0.2600	250
F111PUHP2	0.7800	FULL	0.2600	216
F111PUIP2	1.0000	0.3189	0.2600	211
F111PUJP2	1.0000	0.2600	0.2600	222
F111PUKP2	1.0000	0.2000	0.2600	227

Table 3: Finite Element Data Structure of Parametric Analysis Matrix.  
Continued

PLASTIC UNREINFORCED MODELS (UNIFIED CONSTITUTIVE): SIP III				
DATA FILE NAME	GRINDOUT RADIUS (Inches)	STIFFENER HEIGHT (Inches)	PLATE THICKNESS (Inches)	MAX VON MISES <u>RESIDUAL</u> STRESS (ksi)
F111PUNFL	0.1575	0.3689	0.2894	145
F111PUANFL	0.4500	0.3189	0.2894	117
F111PUBBNFL	0.4500	0.2600	0.2894	120
F111PUCNFL	0.4500	0.2000	0.2894	127
F111PUDNFL	0.4500	FULL	0.2894	124
F111PUENFL	0.7800	0.3189	0.2894	104
F111PUFNFL	0.7800	0.2600	0.2894	97
F111PUGNFL	0.7800	0.2000	0.2894	102
F111PUHNFL	0.7800	FULL	0.2894	93
F111PUINFL	1.0000	0.3189	0.2894	87
F111PUJNFL	1.0000	0.2600	0.2894	90
F111PUKNFL	1.0000	0.2000	0.2894	90
F111PUP1NFL	0.1575	0.3689	0.3250	122
F111PUAP1NFL	0.4500	0.3189	0.3250	98
F111PUBP1NFL	0.4500	0.2600	0.3250	105
F111PUCP1NFL	0.4500	0.2000	0.3250	106
F111PUDP1NFL	0.4500	FULL	0.3250	102
F111PUEP1NFL	0.7800	0.3189	0.3250	78
F111PUFP1NFL	0.7800	0.2600	0.3250	79
F111PUGP1NFL	0.7800	0.2000	0.3250	79
F111PUHP1NFL	0.7800	FULL	0.3250	74
F111PUIP1NFL	1.0000	0.3189	0.3250	69
F111PUJP1NFL	1.0000	0.2600	0.3250	71
F111PUKP1NFL	1.0000	0.2000	0.3250	71
F111PUP2NFL	0.1575	0.3689	0.2600	178
F111PUAP2NFL	0.4500	0.3189	0.2600	152
F111PUBP2NFL	0.4500	0.2600	0.2600	157
F111PUCP2NFL	0.4500	0.2000	0.2600	158
F111PUDP2NFL	0.4500	FULL	0.2600	138
F111PUEP2NFL	0.7800	0.3189	0.2600	123
F111PUFP2NFL	0.7800	0.2600	0.2600	128
F111PUGP2NFL	0.7800	0.2000	0.2600	129
F111PUHP2NFL	0.7800	FULL	0.2600	115
F111PUIP2NFL	1.0000	0.3189	0.2600	112
F111PUJP2NFL	1.0000	0.2600	0.2600	117
F111PUKP2NFL	1.0000	0.2000	0.2600	118

Table 3: Finite Element Data Structure of Parametric Analysis Matrix.  
Continued

ELASTIC UNREINFORCED MODELS: 7.3 g				
DATA FILE NAME	GRINDOUT RADIUS (Inches)	STIFFENER HEIGHT (Inches)	PLATE THICKNESS (Inches)	MAXIMUM VON MISES STRESS (ksi)
F111EU	0.1575	0.3689	0.2894	616
F111EUA	0.4500	0.3189	0.2894	501
F111EUB	0.4500	0.2600	0.2894	513
F111EUC	0.4500	0.2000	0.2894	514
F111EUD	0.4500	FULL	0.2894	466
F111EUE	0.7800	0.3189	0.2894	430
F111EUF	0.7800	0.2600	0.2894	439
F111EUG	0.7800	0.2000	0.2894	438
F111EUH	0.7800	FULL	0.2894	411
F111EUI	1.0000	0.3189	0.2894	406
F111EUJ	1.0000	0.2600	0.2894	413
F111EUK	1.0000	0.2000	0.2894	412
F111EUP1	0.1575	0.3689	0.3250	549
F111EUAP1	0.4500	0.3189	0.3250	443
F111EUBP1	0.4500	0.2600	0.3250	451
F111EUCP1	0.4500	0.2000	0.3250	449
F111EUDP1	0.4500	FULL	0.3250	411
F111EUEP1	0.7800	0.3189	0.3250	380
F111EUFP1	0.7800	0.2600	0.3250	385
F111EUGP1	0.7800	0.2000	0.3250	383
F111EUHP1	0.7800	FULL	0.3250	364
F111EUIP1	1.0000	0.3189	0.3250	358
F111EUJP1	1.0000	0.2600	0.3250	361
F111EUKP1	1.0000	0.2000	0.3250	359
F111EUP2	0.1575	0.3689	0.2600	687
F111EUAP2	0.4500	0.3189	0.2600	563
F111EUBP2	0.4500	0.2600	0.2600	581
F111EUCP2	0.4500	0.2000	0.2600	585
F111EUDP2	0.4500	FULL	0.2600	528
F111EUEP2	0.7800	0.3189	0.2600	484
F111EUFP2	0.7800	0.2600	0.2600	499
F111EUGP2	0.7800	0.2000	0.2600	501
F111EUHP2	0.7800	FULL	0.2600	463
F111EUIP2	1.0000	0.3189	0.2600	458
F111EUJP2	1.0000	0.2600	0.2600	469
F111EUKP2	1.0000	0.2000	0.2600	471

Table 3: Finite Element Data Structure of Parametric Analysis Matrix.  
Continued

ELASTIC UNREINFORCED MODELS: -2.4 g				
DATA FILE NAME	GRINDOUT RADIUS (Inches)	STIFFENER HEIGHT (Inches)	PLATE THICKNESS (Inches)	MAXIMUM VON MISES STRESS (ksi)
F111EU2	0.1575	0.3689	0.2894	202
F111EU2A	0.4500	0.3189	0.2894	164
F111EU2B	0.4500	0.2600	0.2894	168
F111EU2C	0.4500	0.2000	0.2894	168
F111EU2D	0.4500	FULL	0.2894	153
F111EU2E	0.7800	0.3189	0.2894	141
F111EU2F	0.7800	0.2600	0.2894	144
F111EU2G	0.7800	0.2000	0.2894	143
F111EU2H	0.7800	FULL	0.2894	134
F111EU2I	1.0000	0.3189	0.2894	133
F111EU2J	1.0000	0.2600	0.2894	135
F111EU2K	1.0000	0.2000	0.2894	135
F111EU2P1	0.1575	0.3689	0.3250	180
F111EU2AP1	0.4500	0.3189	0.3250	145
F111EU2BP1	0.4500	0.2600	0.3250	148
F111EU2CP1	0.4500	0.2000	0.3250	147
F111EU2DP1	0.4500	FULL	0.3250	134
F111EU2EP1	0.7800	0.3189	0.3250	124
F111EU2FP1	0.7800	0.2600	0.3250	126
F111EU2GP1	0.7800	0.2000	0.3250	126
F111EU2HP1	0.7800	FULL	0.3250	119
F111EU2IP1	1.0000	0.3189	0.3250	118
F111EU2JP1	1.0000	0.2600	0.3250	118
F111EU2KP1	1.0000	0.2000	0.3250	118
F111EU2P2	0.1575	0.3689	0.2600	225
F111EU2AP2	0.4500	0.3189	0.2600	184
F111EU2BP2	0.4500	0.2600	0.2600	190
F111EU2CP2	0.4500	0.2000	0.2600	191
F111EU2DP2	0.4500	FULL	0.2600	173
F111EU2EP2	0.7800	0.3189	0.2600	158
F111EU2FP2	0.7800	0.2600	0.2600	163
F111EU2GP2	0.7800	0.2000	0.2600	164
F111EU2HP2	0.7800	FULL	0.2600	151
F111EU2IP2	1.0000	0.3189	0.2600	150
F111EU2JP2	1.0000	0.2600	0.2600	154
F111EU2KP2	1.0000	0.2000	0.2600	154

Table 3: Finite Element Data Structure of Parametric Analysis Matrix.  
Continued

ELASTIC REINFORCED MODELS: 7.33 g, 1.3° kink angle				
DATA FILE NAME	GRINDOUT RADIUS (Inches)	STIFFENER HEIGHT (Inches)	PLATE THICKNESS (Inches)	MAXIMUM VON MISES STRESS (ksi)
F111ERK3	0.1575	0.3689	0.2894	366
F111ERK3A	0.4500	0.3189	0.2894	292
F111ERK3B	0.4500	0.2600	0.2894	294
F111ERK3C	0.4500	0.2000	0.2894	291
F111ERK3D	0.4500	FULL	0.2894	216
F111ERK3E	0.7800	0.3189	0.2894	250
F111ERK3F	0.7800	0.2600	0.2894	251
F111ERK3G	0.7800	0.2000	0.2894	246
F111ERK3H	0.7800	FULL	0.2894	193
F111ERK3I	1.0000	0.3189	0.2894	236
F111ERK3J	1.0000	0.2600	0.2894	235
F111ERK3K	1.0000	0.2000	0.2894	232
F111ERK3P1	0.1575	0.3689	0.3250	345
F111ERK3AP1	0.4500	0.3189	0.3250	275
F111ERK3BP1	0.4500	0.2600	0.3250	277
F111ERK3CP1	0.4500	0.2000	0.3250	274
F111ERK3DP1	0.4500	FULL	0.3250	211
F111ERK3EP1	0.7800	0.3189	0.3250	236
F111ERK3FP1	0.7800	0.2600	0.3250	236
F111ERK3GP1	0.7800	0.2000	0.3250	233
F111ERK3HP1	0.7800	FULL	0.3250	189
F111ERK3IP1	1.0000	0.3189	0.3250	222
F111ERK3JP1	1.0000	0.2600	0.3250	222
F111ERK3KP1	1.0000	0.2000	0.3250	218
F111ERK3P2	0.1575	0.3689	0.2600	375
F111ERK3AP2	0.4500	0.3189	0.2600	300
F111ERK3BP2	0.4500	0.2600	0.2600	303
F111ERK3CP2	0.4500	0.2000	0.2600	301
F111ERK3DP2	0.4500	FULL	0.2600	216
F111ERK3EP2	0.7800	0.3189	0.2600	257
F111ERK3FP2	0.7800	0.2600	0.2600	259
F111ERK3GP2	0.7800	0.2000	0.2600	256
F111ERK3HP2	0.7800	FULL	0.2600	194
F111ERK3IP2	1.0000	0.3189	0.2600	243
F111ERK3JP2	1.0000	0.2600	0.2600	242
F111ERK3KP2	1.0000	0.2000	0.2600	240

Table 3: Finite Element Data Structure of Parametric Analysis Matrix.  
Continued

ELASTIC REINFORCED MODELS: -2.4 g, 1.3° kink angle				
DATA FILE NAME	GRINDOUT RADIUS (Inches)	STIFFENER HEIGHT (Inches)	PLATE THICKNESS (Inches)	MAXIMUM VON MISES STRESS (ksi)
F111ER2K3	0.1575	0.3689	0.2894	112
F111ER2K3A	0.4500	0.3189	0.2894	89
F111ER2K3B	0.4500	0.2600	0.2894	90
F111ER2K3C	0.4500	0.2000	0.2894	89
F111ER2K3D	0.4500	FULL	0.2894	65
F111ER2K3E	0.7800	0.3189	0.2894	76
F111ER2K3F	0.7800	0.2600	0.2894	77
F111ER2K3G	0.7800	0.2000	0.2894	76
F111ER2K3H	0.7800	FULL	0.2894	58
F111ER2K3I	1.0000	0.3189	0.2894	72
F111ER2K3J	1.0000	0.2600	0.2894	72
F111ER2K3K	1.0000	0.2000	0.2894	71
F111ER2K3P1	0.1575	0.3689	0.3250	105
F111ER2K3AP1	0.4500	0.3189	0.3250	84
F111ER2K3BP1	0.4500	0.2600	0.3250	84
F111ER2K3CP1	0.4500	0.2000	0.3250	84
F111ER2K3DP1	0.4500	FULL	0.3250	63
F111ER2K3EP1	0.7800	0.3189	0.3250	72
F111ER2K3FP1	0.7800	0.2600	0.3250	72
F111ER2K3GP1	0.7800	0.2000	0.3250	71
F111ER2K3HP1	0.7800	FULL	0.3250	57
F111ER2K3IP1	1.0000	0.3189	0.3250	68
F111ER2K3JP1	1.0000	0.2600	0.3250	68
F111ER2K3KP1	1.0000	0.2000	0.3250	66
F111ER2K3P2	0.1575	0.3689	0.2600	115
F111ER2K3AP2	0.4500	0.3189	0.2600	92
F111ER2K3BP2	0.4500	0.2600	0.2600	94
F111ER2K3CP2	0.4500	0.2000	0.2600	93
F111ER2K3DP2	0.4500	FULL	0.2600	66
F111ER2K3EP2	0.7800	0.3189	0.2600	79
F111ER2K3FP2	0.7800	0.2600	0.2600	80
F111ER2K3GP2	0.7800	0.2000	0.2600	79
F111ER2K3HP2	0.7800	FULL	0.2600	59
F111ER2K3IP2	1.0000	0.3189	0.2600	75
F111ER2K3JP2	1.0000	0.2600	0.2600	75
F111ER2K3KP2	1.0000	0.2000	0.2600	74

Table 3: Finite Element Data Structure of Parametric Analysis Matrix.  
Continued

ELASTIC REINFORCED MODELS (UNIFIED CONSTITUTIVE): 1.3° kink angle, SIP III				
DATA FILE NAME	GRINDOUT RADIUS (Inches)	STIFFENER HEIGHT (Inches)	PLATE THICKNESS (Inches)	MAX VON MISES <u>RESIDUAL STRESS</u> (ksi)
F111ERK3NFL	0.1575	0.3689	0.2894	77
F111ERK3ANFL	0.4500	0.3189	0.2894	57
F111ERK3BNFL	0.4500	0.2600	0.2894	58
F111ERK3CNFL	0.4500	0.2000	0.2894	54
F111ERK3DNFL	0.4500	FULL	0.2894	37
F111ERK3ENFL	0.7800	0.3189	0.2894	46
F111ERK3FNFL	0.7800	0.2600	0.2894	47
F111ERK3GNFL	0.7800	0.2000	0.2894	46
F111ERK3HNFL	0.7800	FULL	0.2894	18
F111ERK3INFL	1.0000	0.3189	0.2894	40
F111ERK3JNFL	1.0000	0.2600	0.2894	41
F111ERK3KNFL	1.0000	0.2000	0.2894	38
F111ERK3P1NFL	0.1575	0.3689	0.3250	71
F111ERK3AP1NFL	0.4500	0.3189	0.3250	52
F111ERK3BP1NFL	0.4500	0.2600	0.3250	54
F111ERK3CP1NFL	0.4500	0.2000	0.3250	53
F111ERK3DP1NFL	0.4500	FULL	0.3250	33
F111ERK3EP1NFL	0.7800	0.3189	0.3250	40
F111ERK3FP1NFL	0.7800	0.2600	0.3250	40
F111ERK3GP1NFL	0.7800	0.2000	0.3250	40
F111ERK3HP1NFL	0.7800	FULL	0.3250	15
F111ERK3IP1NFL	1.0000	0.3189	0.3250	34
F111ERK3JP1NFL	1.0000	0.2600	0.3250	33
F111ERK3KP1NFL	1.0000	0.2000	0.3250	32
F111ERK3P2NFL	0.1575	0.3689	0.2600	79
F111ERK3AP2NFL	0.4500	0.3189	0.2600	59
F111ERK3BP2NFL	0.4500	0.2600	0.2600	60
F111ERK3CP2NFL	0.4500	0.2000	0.2600	60
F111ERK3DP2NFL	0.4500	FULL	0.2600	36
F111ERK3EP2NFL	0.7800	0.3189	0.2600	47
F111ERK3FP2NFL	0.7800	0.2600	0.2600	48
F111ERK3GP2NFL	0.7800	0.2000	0.2600	44
F111ERK3HP2NFL	0.7800	FULL	0.2600	20
F111ERK3IP2NFL	1.0000	0.3189	0.2600	43
F111ERK3JP2NFL	1.0000	0.2600	0.2600	41
F111ERK3KP2NFL	1.0000	0.2000	0.2600	42

*Table 4: Unreinforced elastic finite element calibration Bending to Axial ratio results at 50% of load case.*

Load Case	6L	9L	AXIAL	BEND	RATIO	DIFF	COMMENT
7.3g	-959	-5216	-3088	-2129	0.689		USAF CPLT
7.3g	-777	-5262	-3020	-2243	0.743	7.8	Finite Element
-2.4g	433	1645	1039	606	0.583		USAF CPLT
-2.4g	365	1481	923	558	0.605	3.7	Finite Element

All strain values in microstrain.

All DIFF values in percent.

Table 5: Reinforced elastic finite element calibration Bending to Axial ratio results at 100% load for A8-113.

Load	PFDS	LWS32b	LWR10a	AXIAL1	AXIAL2	BEND1	BEND2	ratio1	ratio2	DIFF1	DIFF2	COMMENT
7.33 <sup>g</sup>	-2135	-7079	-2911	-4607	-4995	-2472	-2084	.537	.417			A8-113 CPLT
7.33 <sup>g</sup>	-1697	-8401	-3441	-5049	-5921	-3352	-2480	.664	.419	-23.6	-4	Base model (BM)
7.33 <sup>g</sup>	-1725	-8091	-3348	-4908	-5720	-3183	-2372	.649	.415	-20.8	.6	BM + Adhesive filler (AF)
7.33 <sup>g</sup>	-2231	-7235	-3181	-4733	-5208	-2502	-2027	.529	.389	1.6	6.7	BM + 'kink' angle 30° (KA30)
7.33 <sup>g</sup>	-2259	-7074	-3107	-4667	-5091	-2408	-1984	.516	.390	3.9	6.6	BM + AF + KA30 (BM1)
7.33 <sup>g</sup>	-2605	-6350	-2932	-4478	-4641	-1873	-1709	.418	.368	22.1	11.7	BM + AF + KA50
-2.4 <sup>g</sup>	862	2266	921	1564	1594	702	673	.449	.422			A8-113 CPLT
-2.4 <sup>g</sup>	740	2316	1018	1528	1667	738	649	.516	.389	-14.9	7.7	BM1 with Load scaled (LS)
-2.4 <sup>g</sup>	771	2201	977	1486	1589	715	612	.481	.385	-7.2	8.7	BM1 + LS + Constants modified
-3.0 <sup>g</sup>	1178	2861	1219	2020	2040	842	821	.417	.402			A8-113 CPLT
-3.0 <sup>g</sup>	924	2896	1272	1910	2084	986	812	.516	.390	-23.8	3.1	BM1 with Load scaled (LS)
-3.0 <sup>g</sup>	964	2751	1221	1858	1986	894	765	.481	.385	-15.4	4.2	BM1 + LS + Constants modified

1 = Calculations based upon gauge PFD5.

2 = Calculations based upon gauge LWR10a.

All strain values in microstrain.

All DIFF values in percent.

## Appendix B: Figures

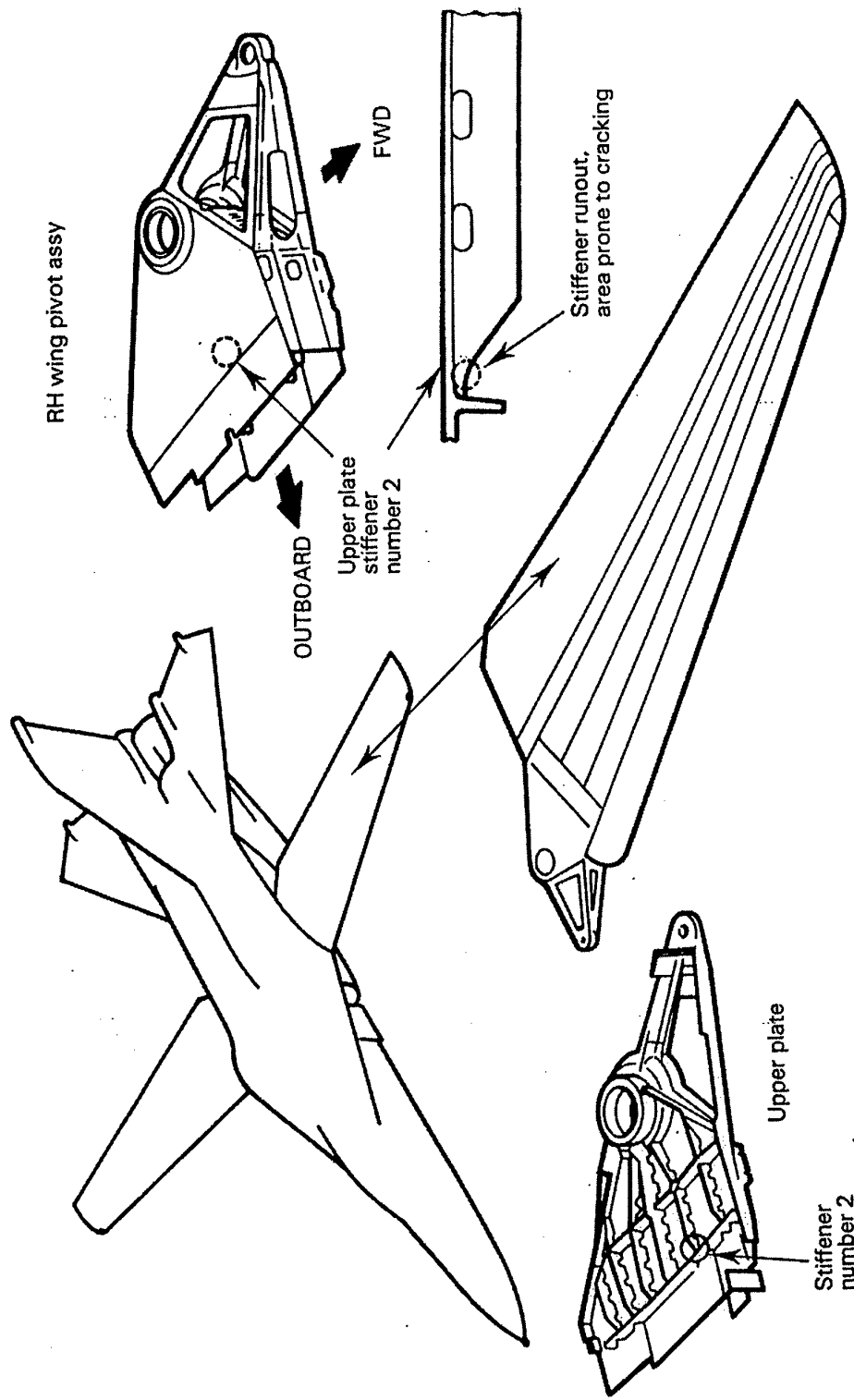


Figure 1: View of F-111 Aircraft and Wing Showing Location of Critical Area.

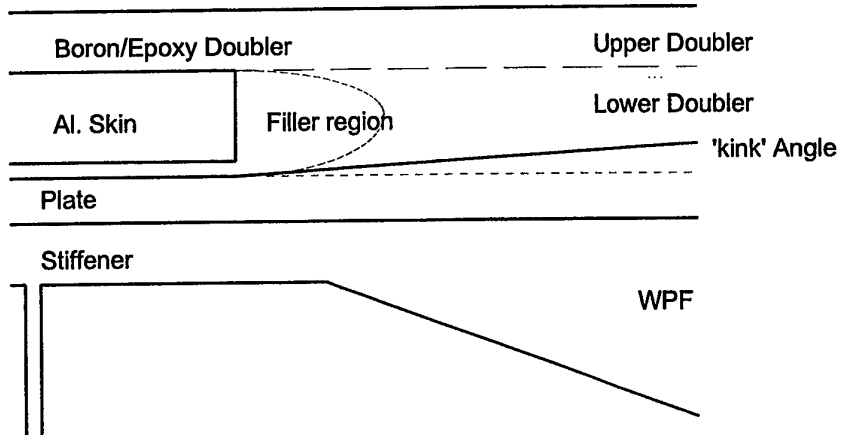


Figure 2: Filler Region and 'kink' Angle definitions.

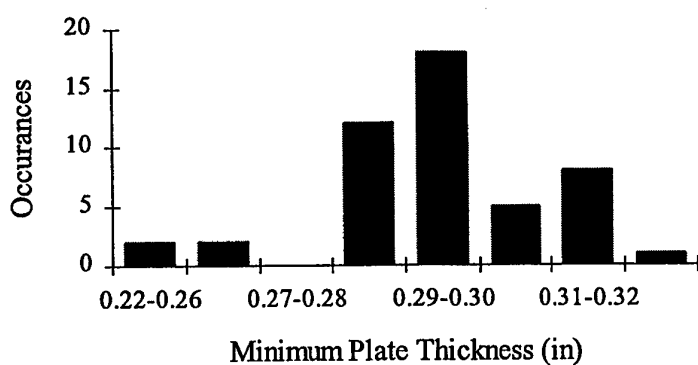


Figure 3: Variation in minimum plate thickness for the F-111 fleet.

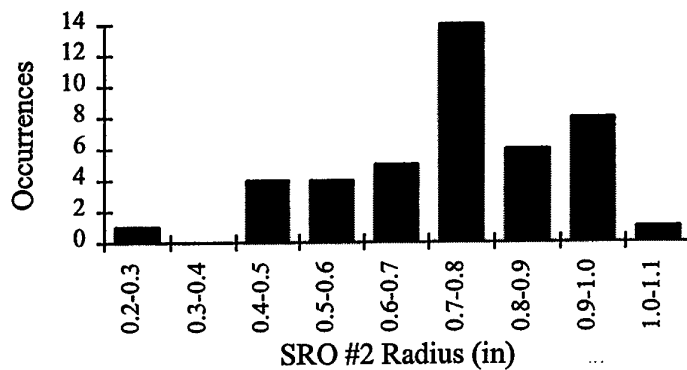


Figure 4: Variation in stiffener runout radius for the F-111 fleet.

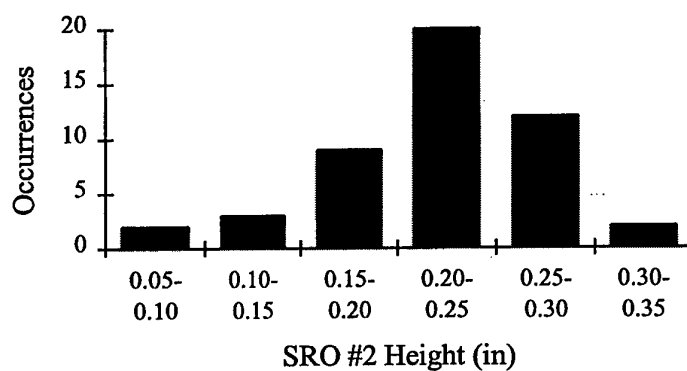


Figure 5: Variation in stiffener height for the F-111 fleet.

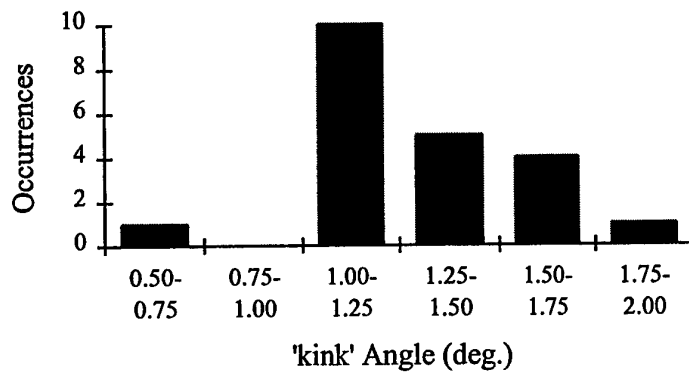


Figure 6: Variation in 'kink' angle for the F-111 wings with doublers.

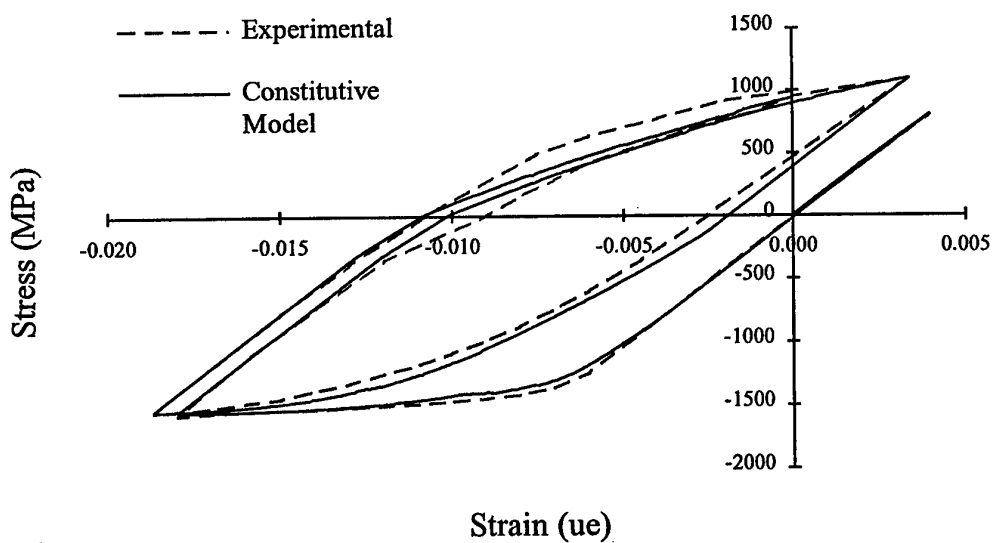


Figure 7: Comparison between Experimental data and generated Unified Constitutive Model data.

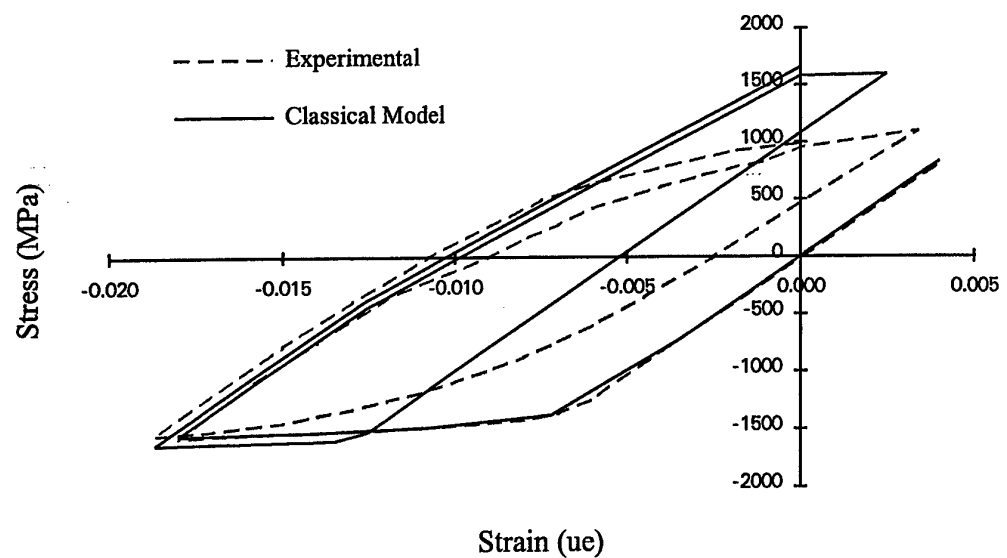
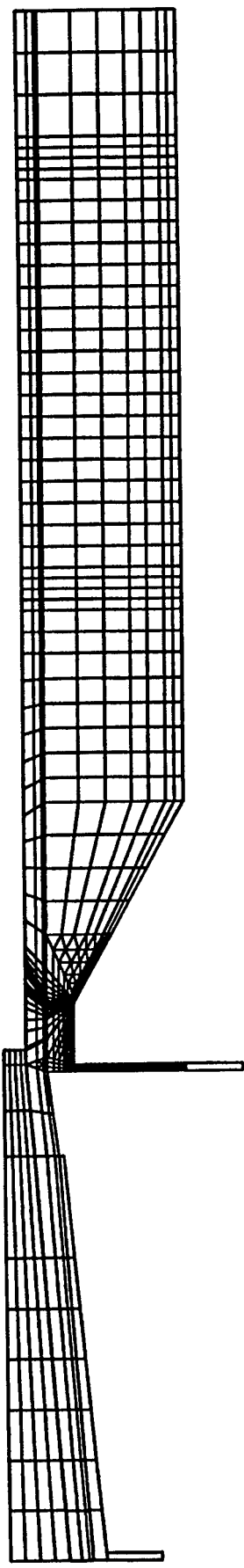


Figure 8: Comparison between Experimental data and generated Classical Model data.



*Figure 9: F-111 SRO#2 Full Finite Element Mesh for Virgin configuration.*

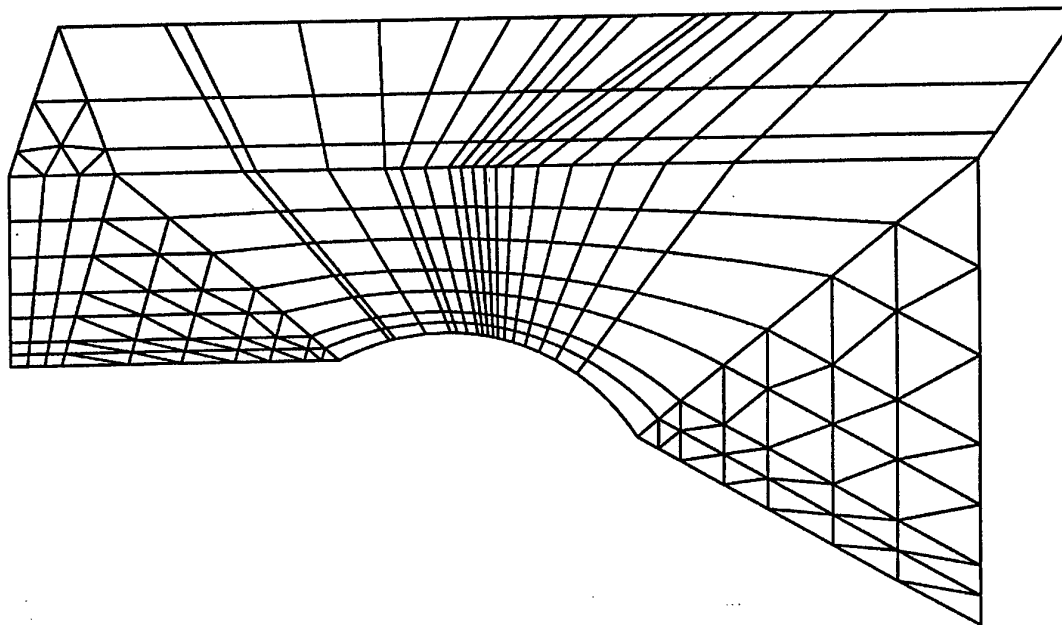


Figure 10: F-111 SRO#2 Mesh Geometry for series A.

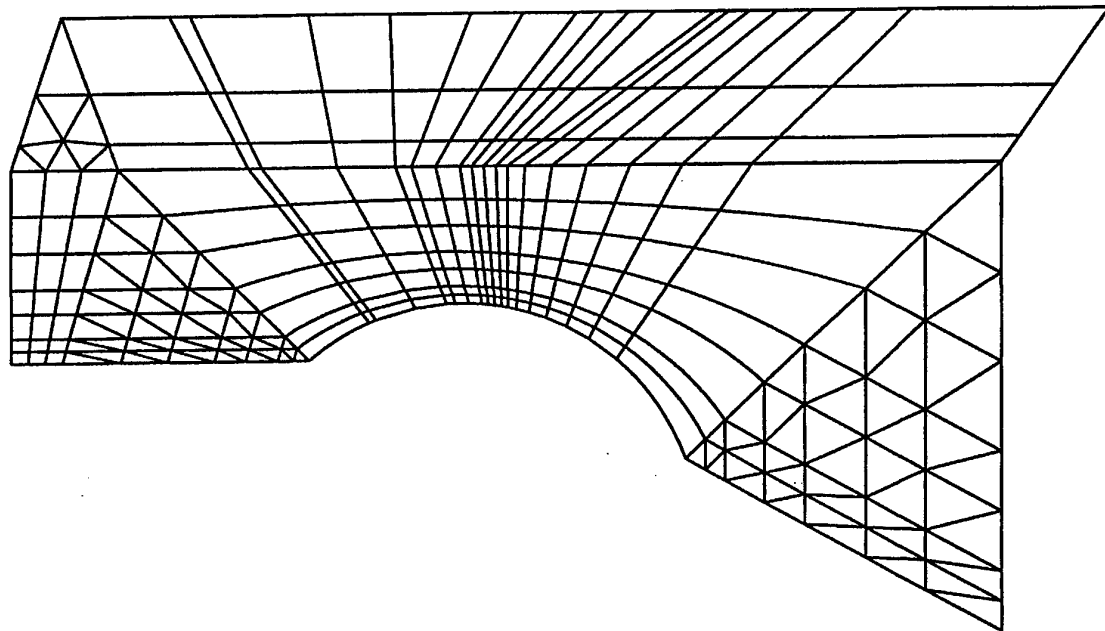


Figure 11: F-111 SRO#2 Mesh Geometry for series B.

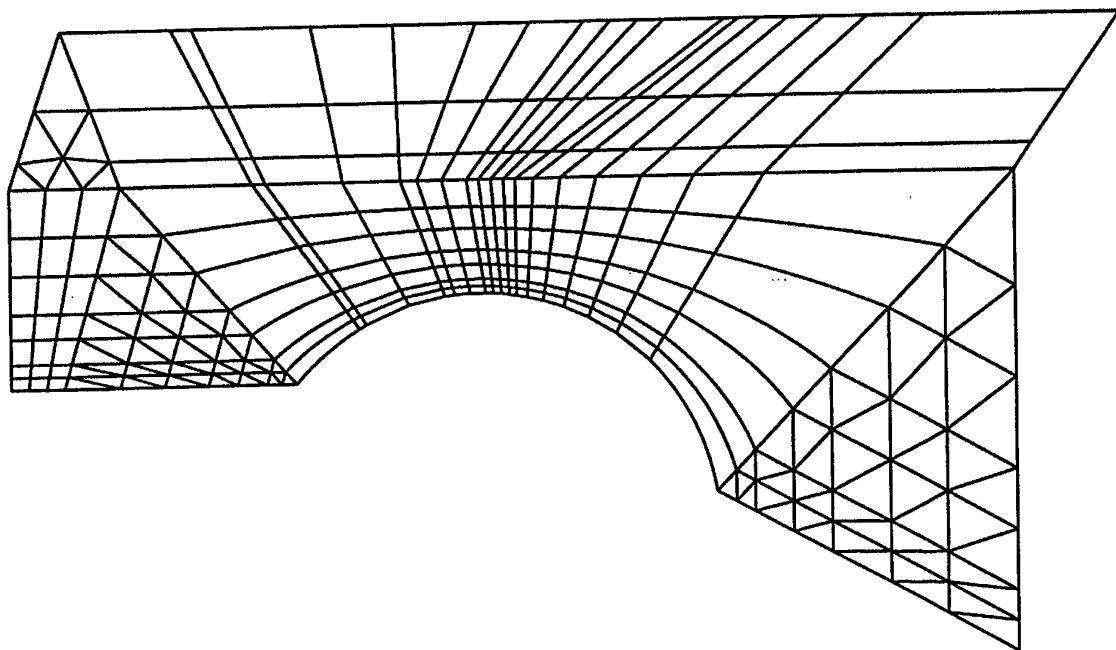


Figure 12: F-111 SRO#2 Mesh Geometry for series C.

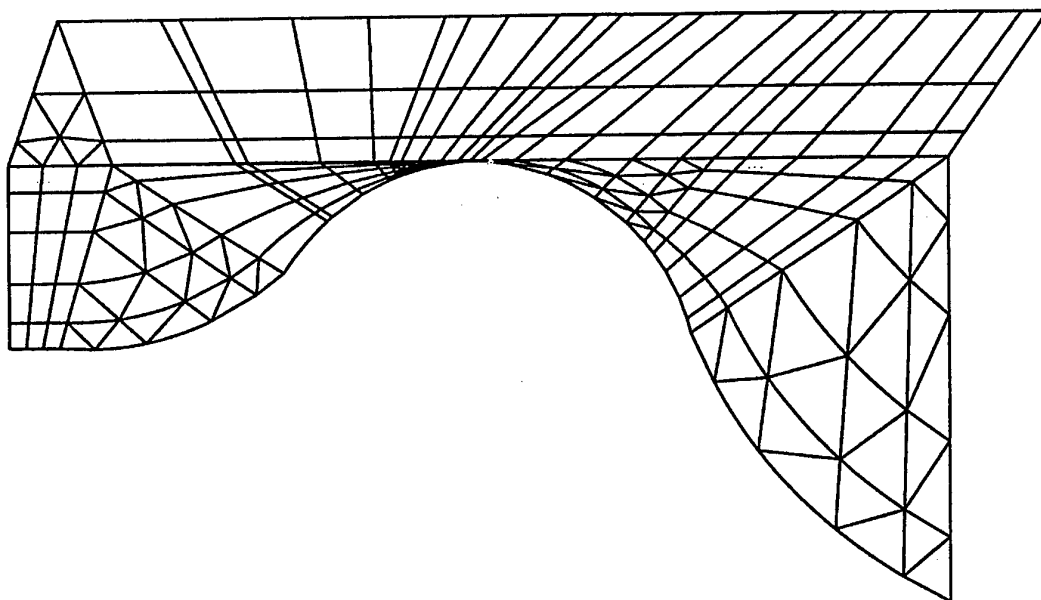


Figure 13: F-111 SRO#2 Mesh Geometry for series D.

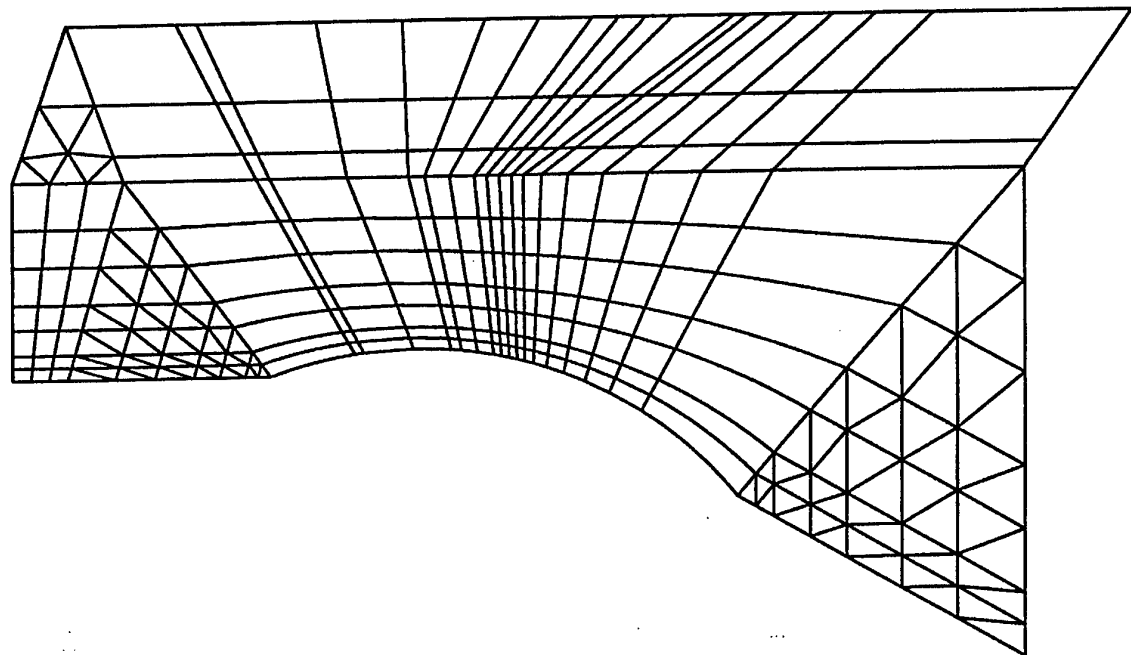


Figure 14: F-111 SRO#2 Mesh Geometry for series E.

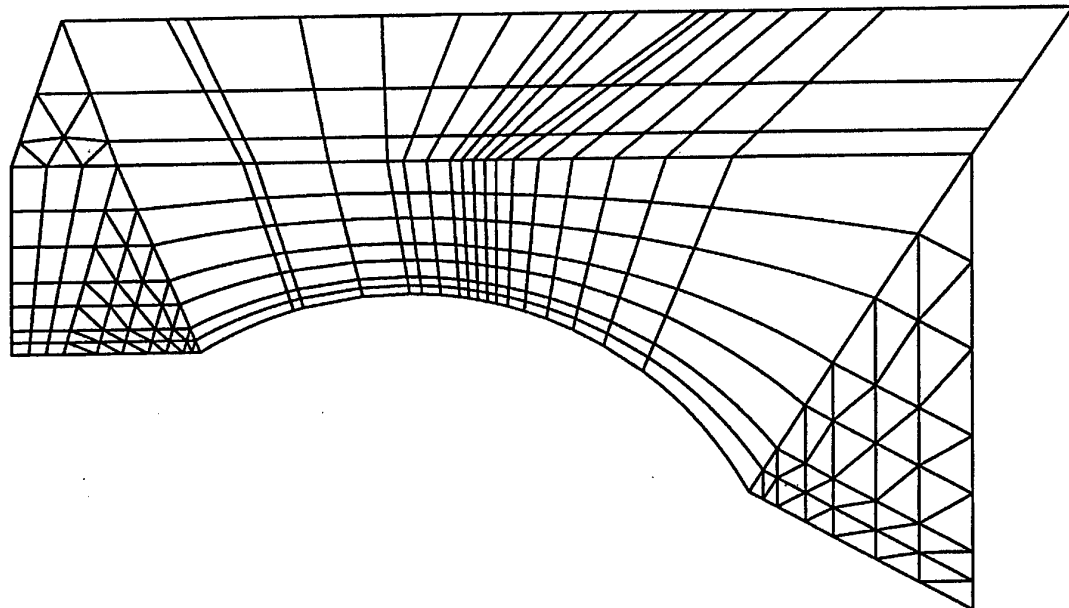


Figure 15: F-111 SRO#2 Mesh Geometry for series F.

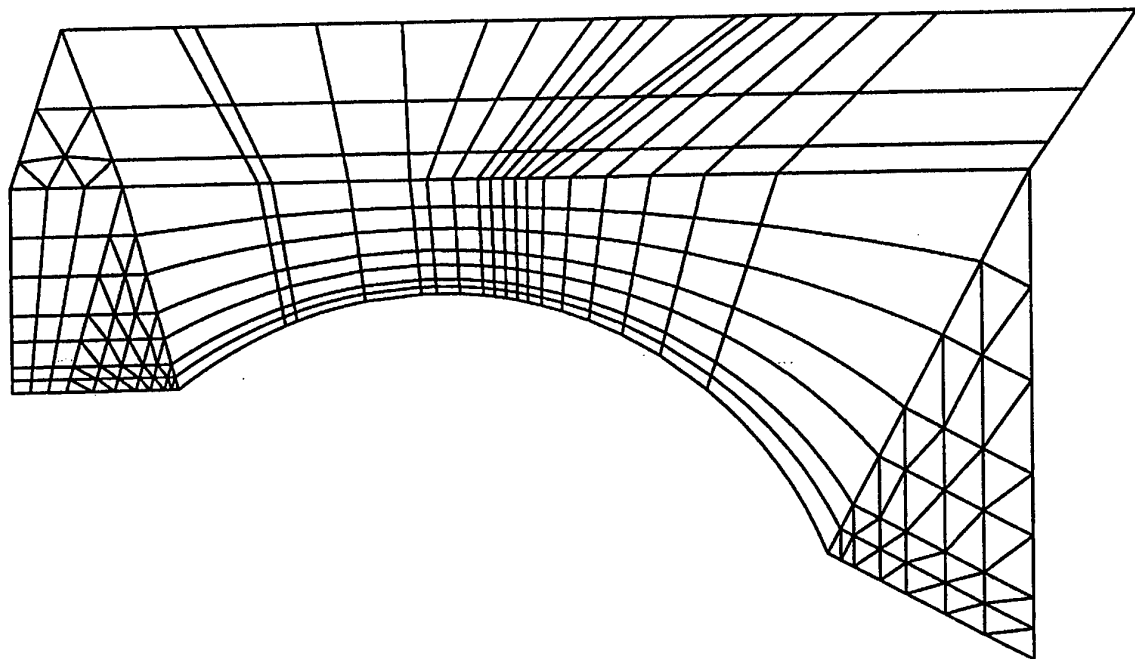


Figure 16: F-111 SRO#2 Mesh Geometry for series G.

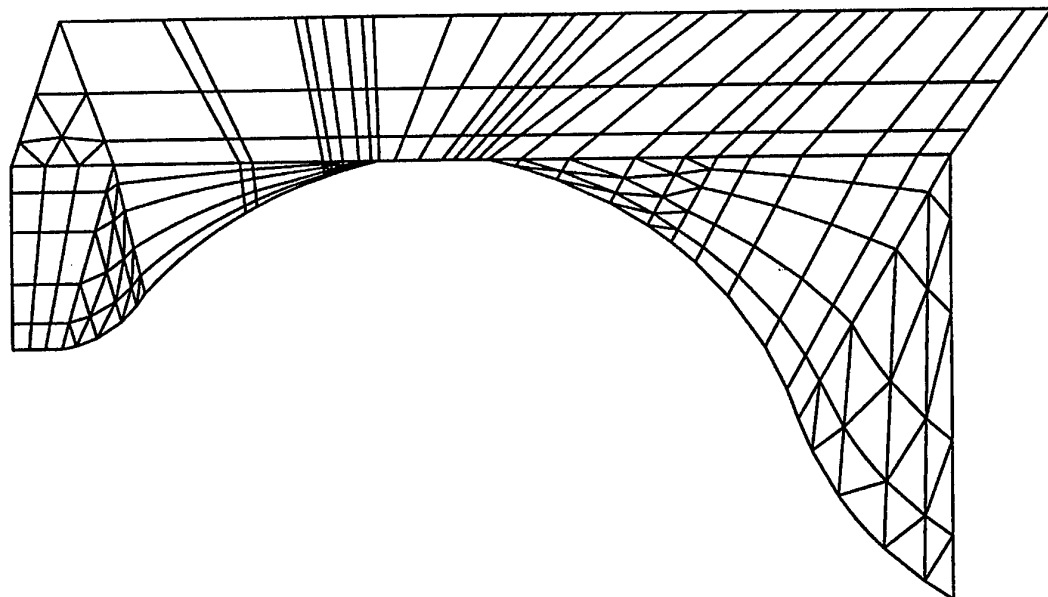


Figure 17: F-111 SRO#2 Mesh Geometry for series H.

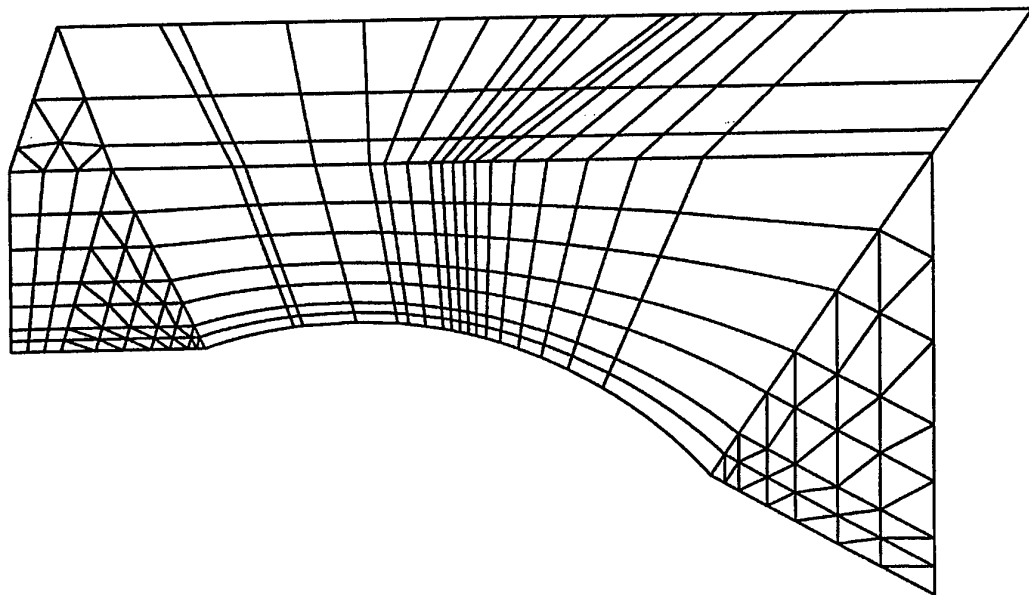


Figure 18: F-111 SRO#2 Mesh Geometry for series I.

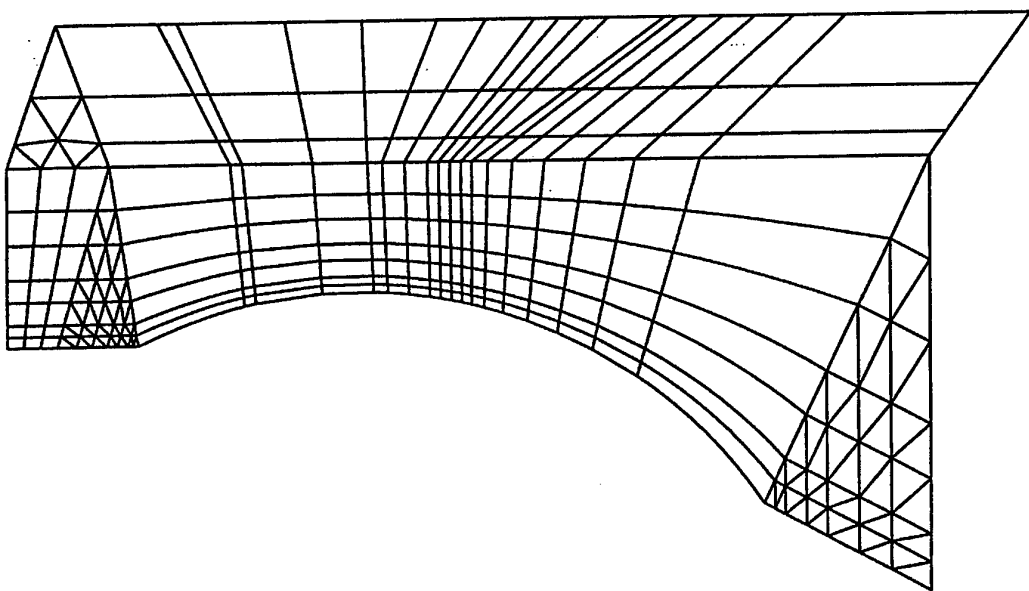
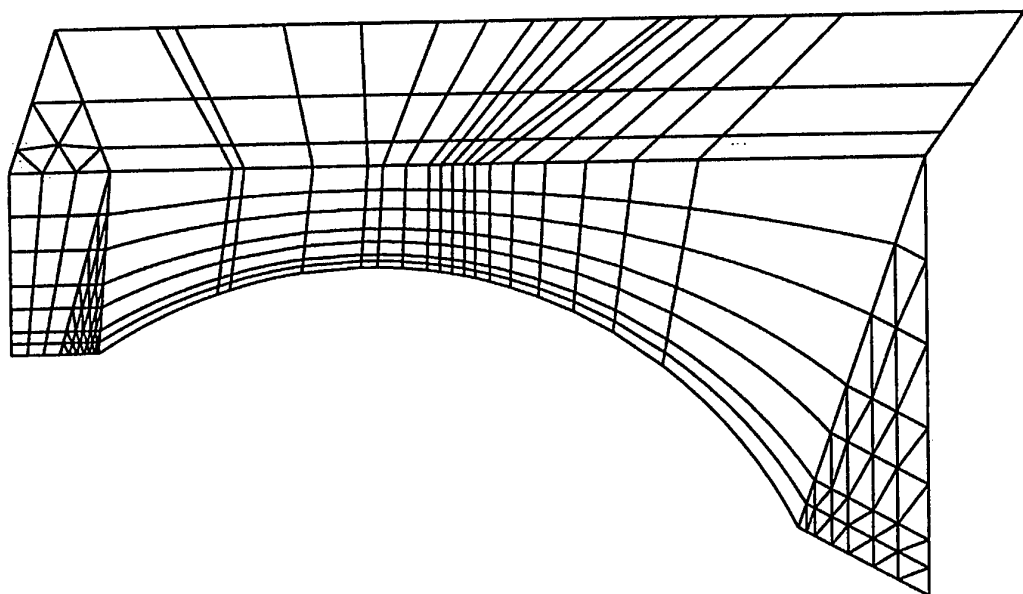
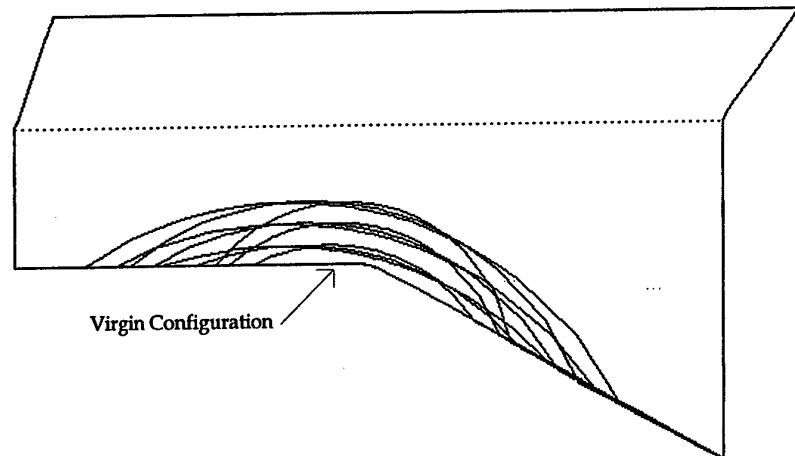


Figure 19: F-111 SRO#2 Mesh Geometry for series J.



*Figure 20: F-111 SRO#2 Mesh Geometry for series K.*



*Figure 21: Parametric geometries for different grind out depths and radii.*

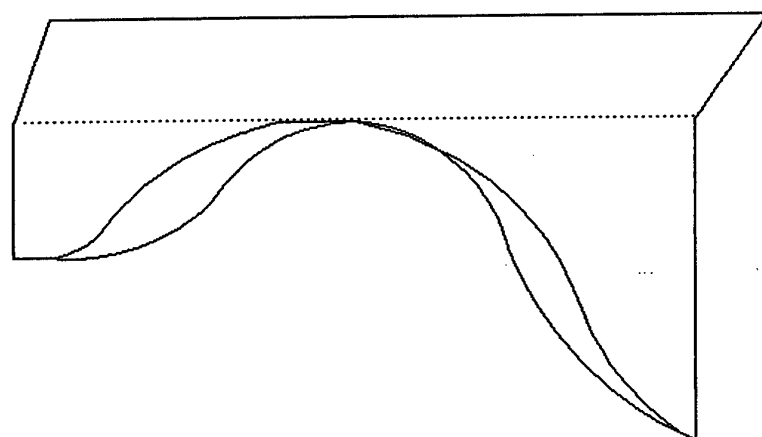


*Figure 22: Full grind out geometry for a 0.45" radius and a 1.00" radius.*

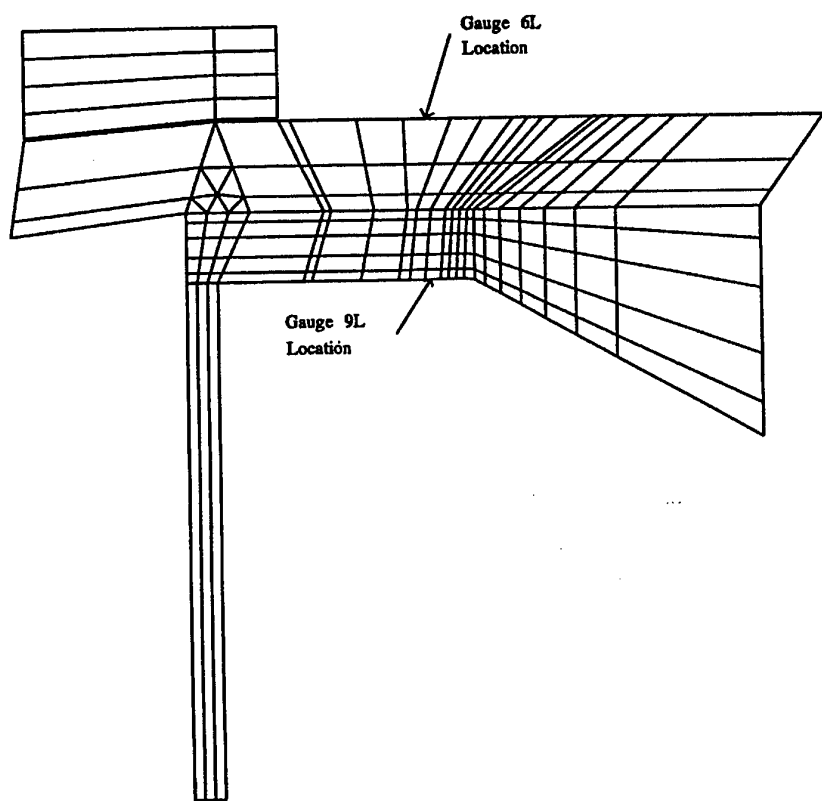
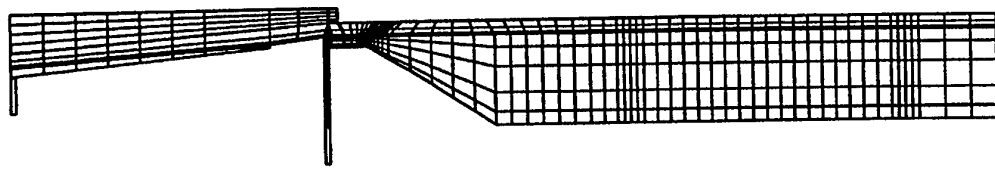


*Figure 23: Finite element mesh of unreinforced USAF calibration model with strain gauge locations.*

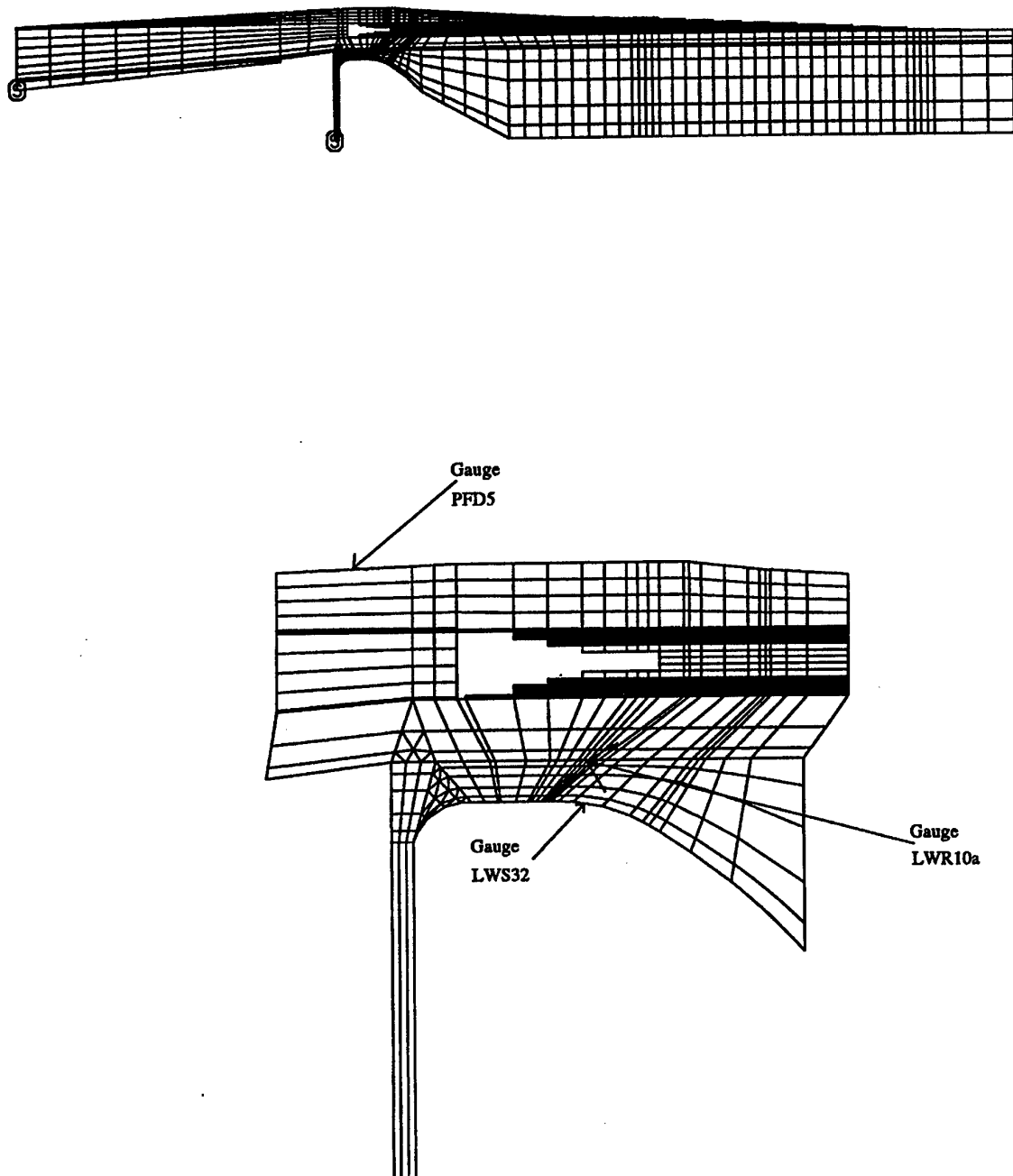
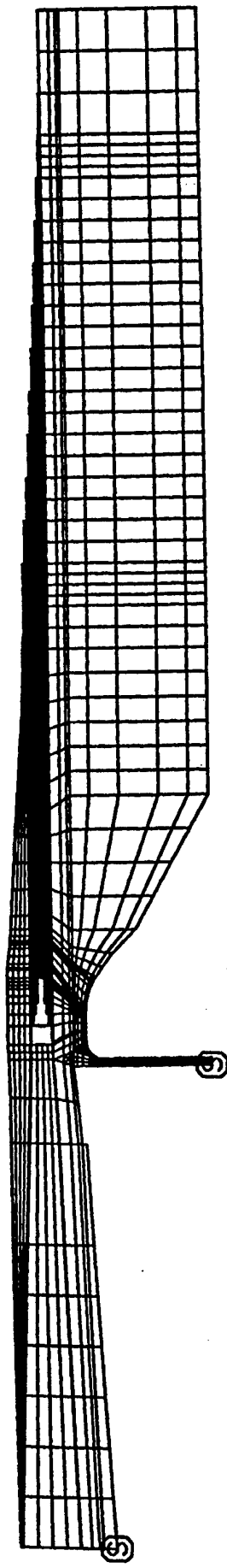


Figure 24: Finite element mesh of reinforced A8-113 calibration model with strain gauge locations at  $0^\circ$  'kink' angle.



DSTO-TN-0104

Figure 25: Finite element mesh of reinforced A8-113 calibration model at 1.97° 'kink' angle.

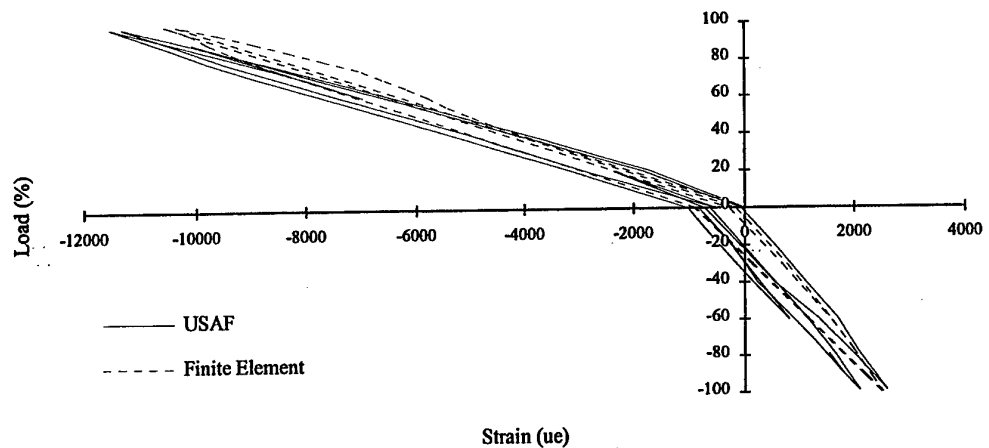


Figure 26: Comparison of USAF wing strain data with unreinforced plastic finite element mesh at gauge 9L.

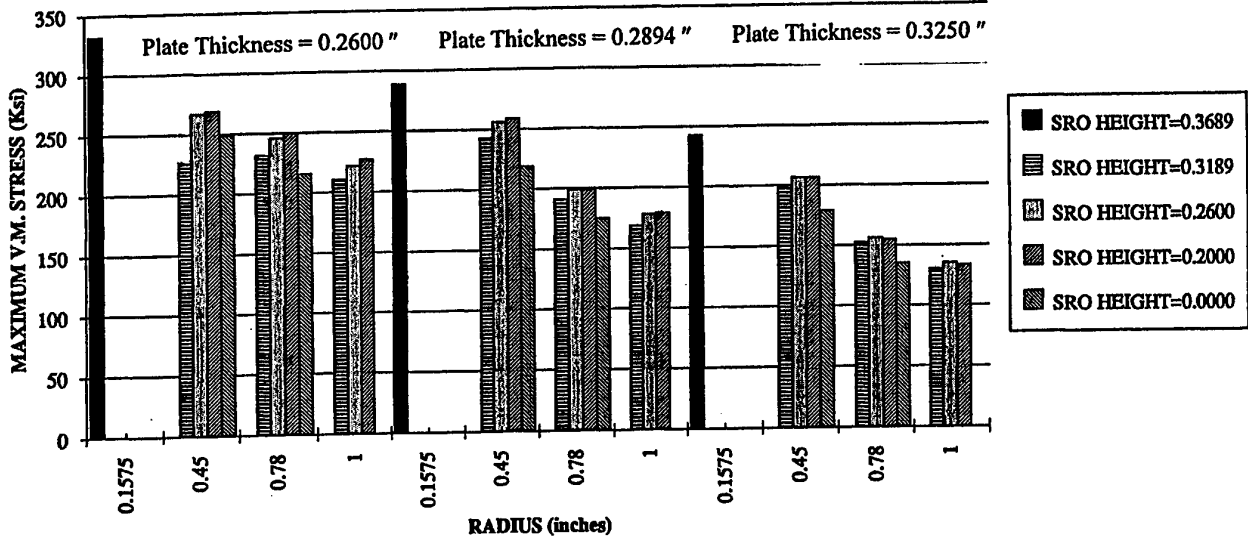


Figure 27: Plastic Unreinforced Analysis (Classical).

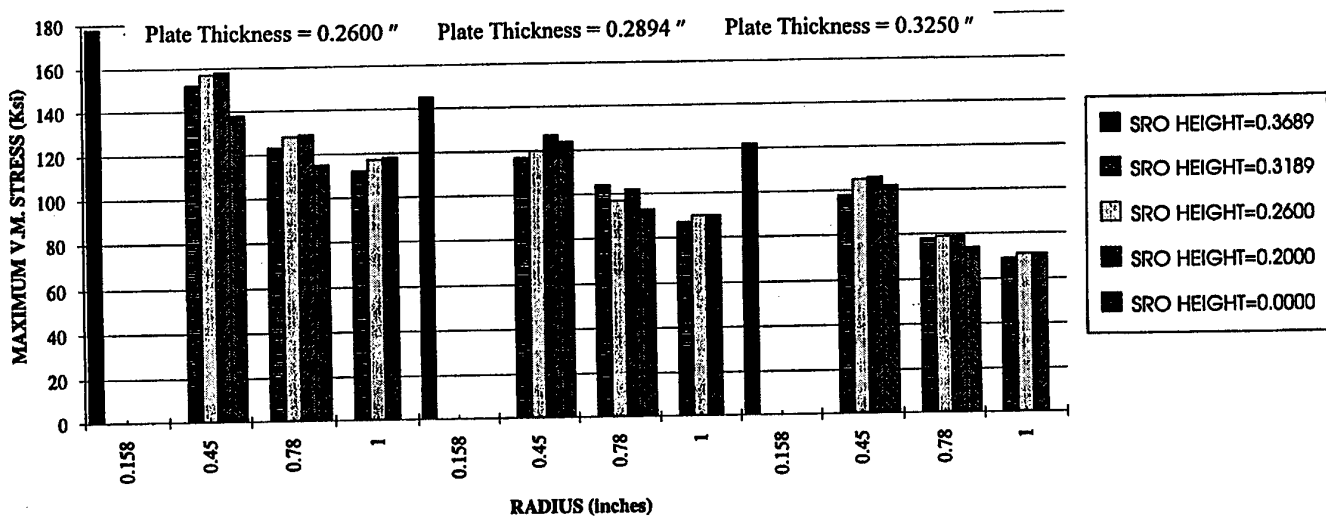


Figure 28: Plastic Unreinforced Analysis (Unified Constitutive)

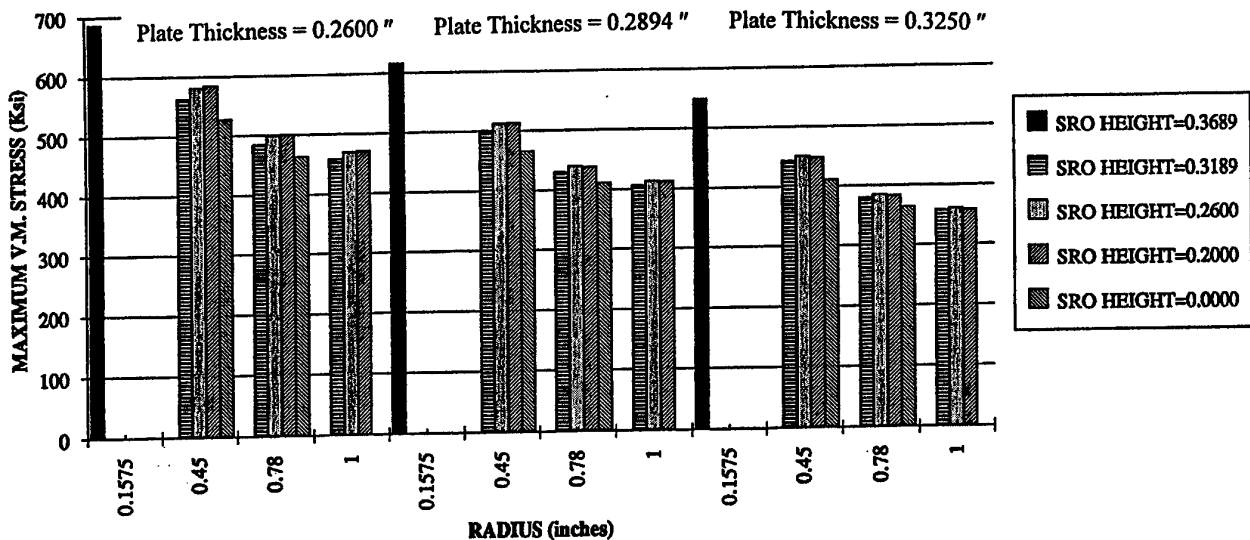


Figure 29: Elastic Unreinforced Analysis (+7.33 g)

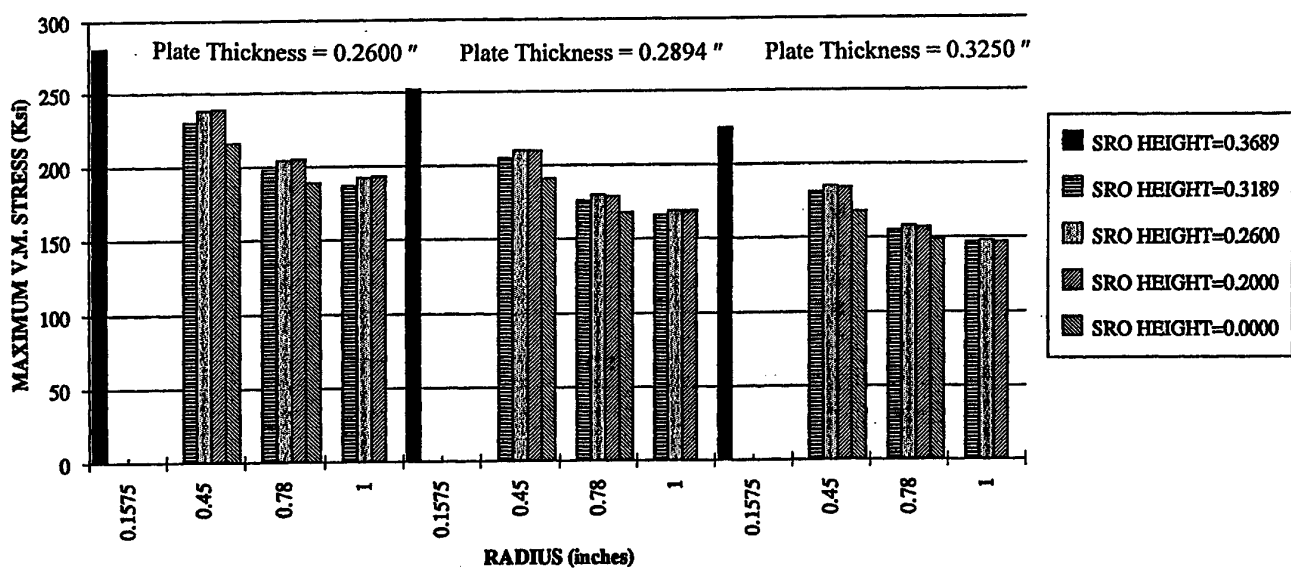


Figure 30: Elastic Unreinforced Analysis (-2.4 g)

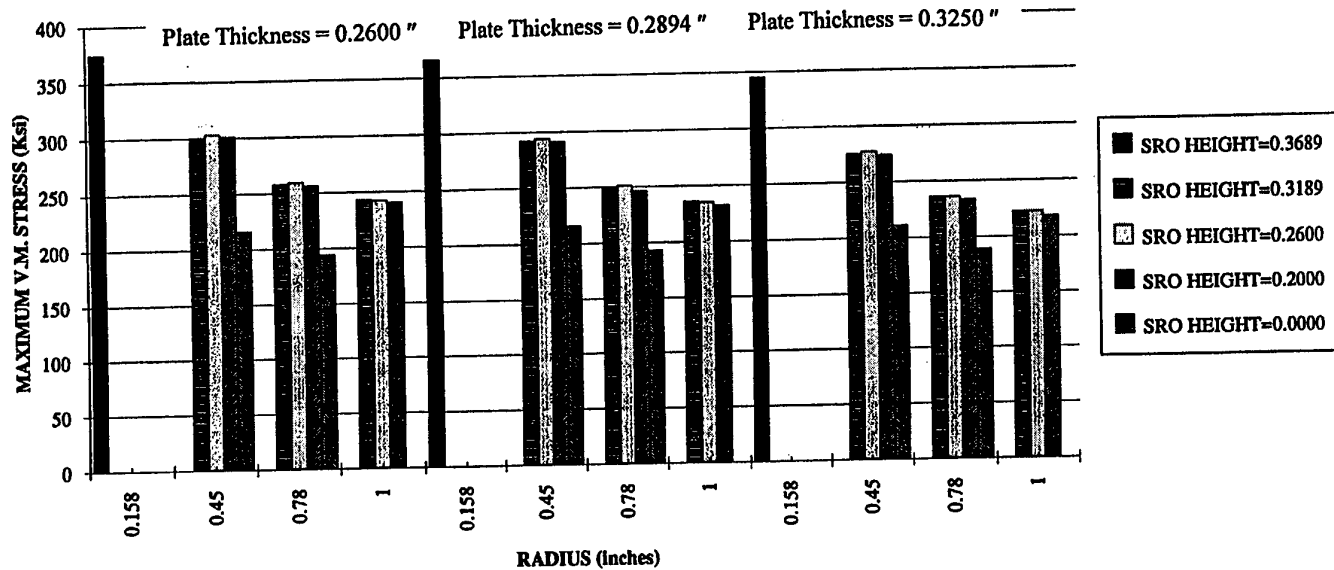


Figure 31: Elastic Reinforced Analysis (+7.33 g, 1.3° 'kink')

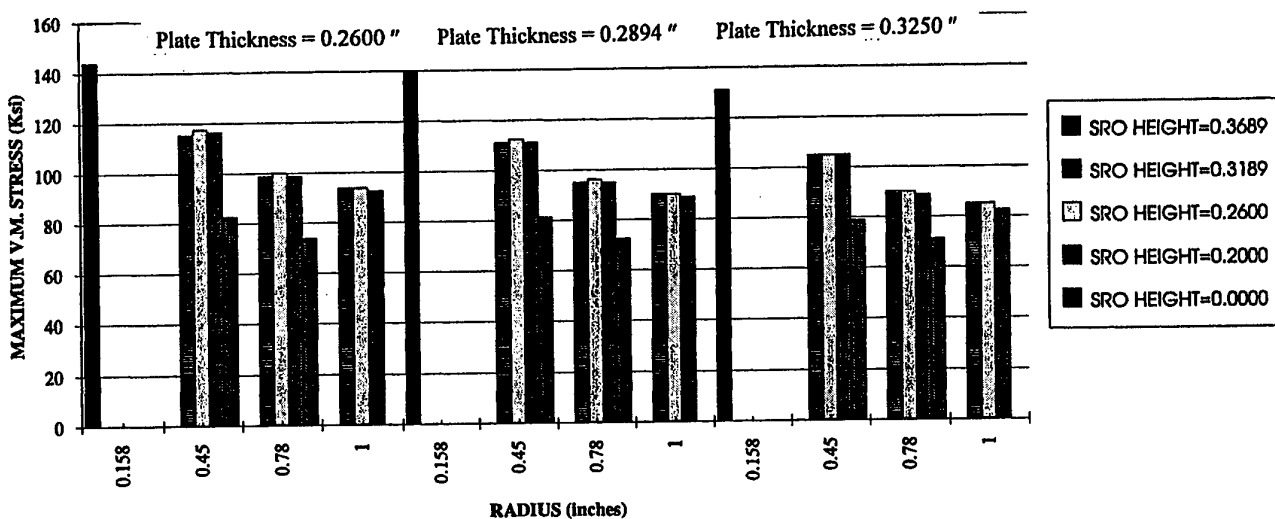


Figure 32: Elastic Reinforced Analysis (-2.4 g, 1.3° 'kink')

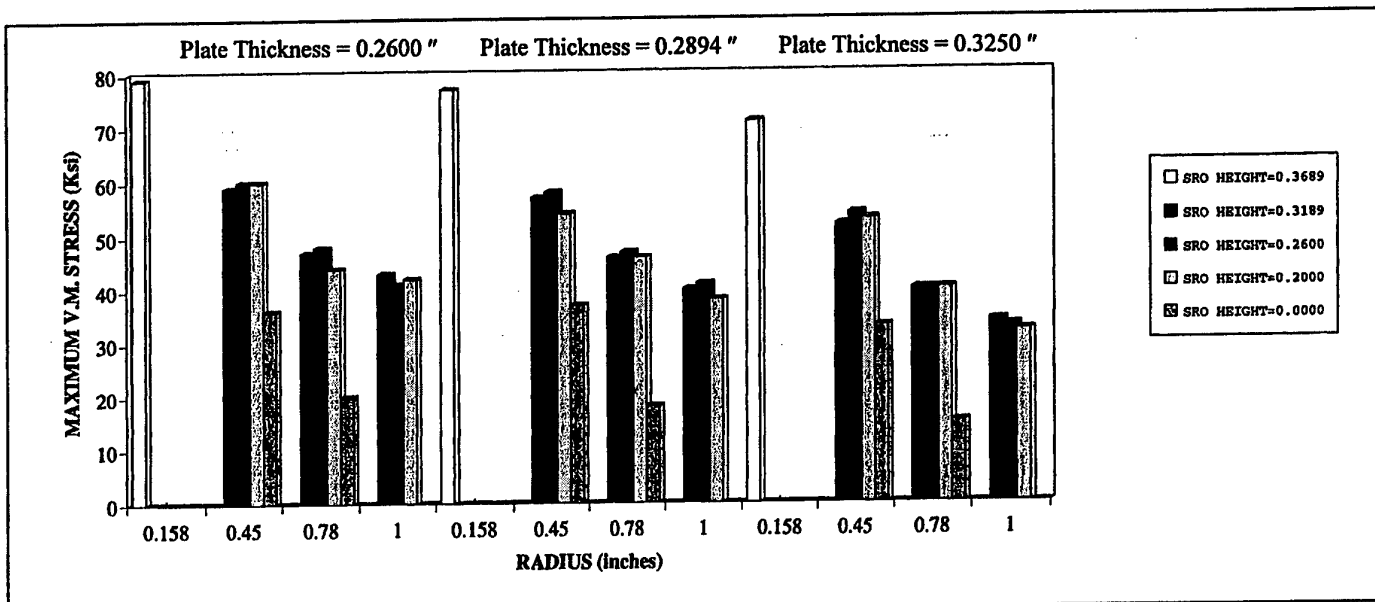


Figure 33: Elastic Reinforced Analysis (Unified Constitutive, Residual Stress, 1.3° 'kink')

## DISTRIBUTION LIST

### F111 Stiffener Run Out #2 Parametric Study

J.Paul

## AUSTRALIA

### DEFENCE ORGANISATION

Task Sponsor DGTA

#### S&T Program

Chief Defence Scientist  
FAS Science Policy  
AS Science Corporate Management } shared copy  
Director General Science Policy Development  
Counsellor Defence Science, London (Doc Data Sheet )  
Counsellor Defence Science, Washington (Doc Data Sheet )  
Scientific Adviser to MRDC Thailand (Doc Data Sheet )  
Navy Scientific Adviser (Doc Data Sheet and distribution list only)  
Scientific Adviser - Army (Doc Data Sheet and distribution list only)  
Air Force Scientific Adviser  
Director Trials

DESRL (Doc Data Sheet and distribution list only)

#### Aeronautical and Maritime Research Laboratory

Director AMRL  
Chief of Airframes and Engines Division  
F. Rose  
K. Watters (5 copies)  
J. Paul (2 copies)

#### DSTO Library and Archives

Library Fishermens Bend  
Library Maribyrnong  
Library Salisbury (2 copies)  
Australian Archives  
Library, MOD, Pyrmont (Doc Data sheet only)  
US Defense Technical Information Center, 2 copies  
UK Defence Research Information Centre, 2 copies  
Canada Defence Scientific Information Service, 1 copy  
NZ Defence Information Centre, 1 copy  
National Library of Australia, 1 copy

**Capability Development Division**

Director General Maritime Development (Doc Data Sheet only)  
Director General Land Development (Doc Data Sheet only)  
Director General C3I Development (Doc Data Sheet only)  
Director General Aerospace Development

**Army**

ABCA Office, G-1-34, Russell Offices, Canberra (4 copies)

**Air Force**

OIC ASI  
ASI2A (2 copies)

**Intelligence Program**

DGSTA Defence Intelligence Organisation  
Manager, Information Centre, Defence Intelligence Organisation

**Corporate Support Program**

OIC TRS, Defence Regional Library, Canberra

**UNIVERSITIES AND COLLEGES**

Australian Defence Force Academy  
Library  
Head of Aerospace and Mechanical Engineering  
Senior Librarian, Hargrave Library, Monash University  
Librarian, Flinders University

**OTHER ORGANISATIONS**

NASA (Canberra)  
Info Australia (formerly AGPS)

**OUTSIDE AUSTRALIA****ABSTRACTING AND INFORMATION ORGANISATIONS**

Library, Chemical Abstracts Reference Service  
Engineering Societies Library, US  
Materials Information, Cambridge Scientific Abstracts, US  
Documents Librarian, The Center for Research Libraries, US

**INFORMATION EXCHANGE AGREEMENT PARTNERS**

Acquisitions Unit, Science Reference and Information Service, UK  
Library - Exchange Desk, National Institute of Standards and Technology, US  
National Aerospace Laboratory, Japan (   
National Aerospace Laboratory, Netherlands  
SPARES (5 copies)

**Total number of copies: 57**

<b>DEFENCE SCIENCE AND TECHNOLOGY ORGANISATION DOCUMENT CONTROL DATA</b>		1. PRIVACY MARKING/CAVEAT (OF DOCUMENT)		
<b>2. TITLE</b> F-111 Stiffener Run Out #2 Parametric Study		<b>3. SECURITY CLASSIFICATION (FOR UNCLASSIFIED REPORTS THAT ARE LIMITED RELEASE USE (L) NEXT TO DOCUMENT CLASSIFICATION)</b> Document (U) Title (U) Abstract (U)		
<b>4. AUTHOR(S)</b> J. Paul		<b>5. CORPORATE AUTHOR</b> Aeronautical and Maritime Research Laboratory PO Box 4331 Melbourne Vic 3001 Australia		
6a. DSTO NUMBER DSTO-TN-0104	6b. AR NUMBER AR-010-301	6c. TYPE OF REPORT Technical Note	7. DOCUMENT DATE October 1999	
8. FILE NUMBER M1/9/393	9. TASK NUMBER AIR96/102	10. TASK SPONSOR DTA-LC	11. NO. OF PAGES 42	12. NO. OF REFERENCES 14
<b>13. DOWNGRADING/DELIMITING INSTRUCTIONS</b>		<b>14. RELEASE AUTHORITY</b> Chief, Airframes and Engines Division		
<b>15. SECONDARY RELEASE STATEMENT OF THIS DOCUMENT</b> <i>Approved for public release</i>				
OVERSEAS ENQUIRIES OUTSIDE STATED LIMITATIONS SHOULD BE REFERRED THROUGH DOCUMENT EXCHANGE, PO BOX 1500, SALISBURY, SA 5108				
<b>16. DELIBERATE ANNOUNCEMENT</b> No Limitations				
<b>17. CASUAL ANNOUNCEMENT</b> Yes <b>18. DEFTEST DESCRIPTORS</b> finite element analysis, plastic deformation, stress relaxation, F-111 aircraft				
<b>19. ABSTRACT</b> The Royal Australian Air Force (RAAF) currently has in service a fleet of F-111 aircraft. The conditions under which the RAAF operates these aircraft have proved to be conducive to cracking in the structurally critical wing pivot fitting, and certification testing in the cold proof load test has demonstrated failures at that location. The RAAF has contracted Lockheed Martin Tactical Aircraft Systems (LMTAS) to perform a Durability And Damage Tolerance Analysis on the aircraft. One control point of concern, in this report, is the Stiffener Run Out Number 2 in the wing pivot fitting. The Aeronautical and Maritime Research Laboratory (AMRL) developed a bonded boron/epoxy reinforcement to reduce the high plastic strains in this critical region, and as a result has significant experience in analysing this region. LMTAS, in conjunction with the RAAF, requested that the AMRL perform an elastic and plastic stress analysis of Stiffener Run Out Number 2 including the effect of varying the geometric parameters associated with it.				